

**Application of Laser Micromachining on Polymeric and
Metallic Substrates**

By

Prashanth Reddy Konari

Master of Science in Engineering Physics-Electrical

Engineering

University of Central Oklahoma

Edmond, Oklahoma

2019

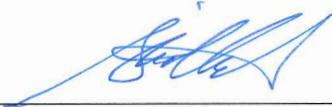
Master Thesis

Submitted to the Faculty of the Graduate College of the
University of Central Oklahoma in partial fulfillment of the
requirements for Degree of Master of Science

June 2019

Application of Laser Micromachining on Polymeric and Metallic Substrates

Thesis Approved:



Committee Chair: Dr. Morshed Khandaker



Committee Member: Dr. Mohammad Hossan



Committee Member: Dr. Scott Mattison

ACKNOWLEDGMENTS

Foremost, I would like to express my sincere gratitude to my advisor Dr. Morshed Khandaker and Dr. Mohammed Hossan for his continuous support, motivation, immense knowledge. Their guidance helped me in all the time of research and writing.

Besides them, I would like to thank the Dr. Scott Mattison for his encouragement and motivation.

My sincere thanks also goes to the Department of Engineering Physics Electrical Engineering and graduate college

Last but not least , I would like to thank my parents for continuously supporting me throughout my life.

Contents

1 Chapter 1	13
1.1 Summary	13
1.2 Laser micromachining	14
1.2.1 Applications of laser Micromachining:.....	14
1.3 Hypothesis	15
1.4 Thesis Statement and objectives.....	15
1.4.1 Objectives.....	17
1.5 Organization of thesis	17
2 Chapter 2.....	18
2.1 Summary	18
2.1.1 Objectives:.....	18
2.2 Microfluidics and its applications:.....	19
2.2.1 Applications of microfluidics:	20
2.3 Conventional techniques and process:	21
2.4 Laser technology:	23
2.4.2 Applications of Laser Ablation Technique:	25
2.5 Laser fabrication of microfluidics:	27
2.6 Materials and Methods:.....	30

2.6.1 Materials:.....	30
2.6.2 Scanning Electron Microscope (SEM)	34
2.6.3 Optical Profilometer.....	35
2.7 Experimental setup and Preparation:	35
2.7.1 Muse laser setup:	35
2.8 Results	37
2.8.1 GLASS:	37
2.8.2 Varying Speed:	39
2.8.3 Varying focal length:	42
2.8.4 Varying Passes:.....	44
2.8.5 Roughness Analysis:	47
2.8.6 Sa (Arithmetical Mean Height)	48
2.9 PMMA:	51
2.9.1 Varying Power:.....	51
2.9.2 Varying focal length:	52
2.9.3 Varying Speed:	54
2.9.4 Varying Pass:.....	56
2.10 PDMS.....	57
2.10.1 Varying Power:.....	58
2.10.2 Varying Focal length:.....	59

2.10.3 Varying Speed:	60
2.10.4 Varying Passes:.....	62
2.10.5 Roughness Analysis:	64
Sa (Arithmetical Mean Height).....	65
2.11 Comparison of PDMS, PMMA and Glass:	66
2.11.1 Width of the cut in terms of varying power:	66
2.11.2 Depth of cut in terms of varying power	67
2.11.3 Width of cut in terms of varying speed	68
2.11.4 Depth of cut interms of varying speed	69
2.11.5 Depth of cut interms of varying focal length.....	70
2.11.6 Width of cut interms of varying focal length:	71
2.11.7 Width of cut interms of varying Pass:.....	72
2.11.8 Depth of cut in terms of varying Pass:	73
2.12 Conclusion:.....	74
3 Chapter 3	76
Effect of laser on Titanium METAL.....	76
3.1 Summary	76
3.2 Introduction	76
3.2.1 Applications of Titanium:	77
3.2.2 Laser applications on titanium:.....	78

3.2.3 Plasma Nitriding on Titanium:	78
.....
3.3 Materials and Methods:	79
3.3.1 Sample Preparation:	80
3.3.2 Chemical state evaluation by X-ray photoelectron spectroscopy (XPS): ..	81
3.4 Results:	82
3.4.1 Topographic analysis:	82
3.4.2 Chemical state analysis:	83
3.4.3 Surface Analysis:	85
3.5 Conclusion:	86
4 Chapter 4	88
4.1 Conclusion:	88
4.2 Future work:	89
4.3 References:	89

LIST OF FIGURES:

Figure 2-1 Crack on walls of PMMA substrate after treating with laser.....	26
Figure 2-2 Bulge formation on walls of PMMA when treated with laser	27
Figure 2-3 direct write laser machining system configuration [28]	28
Figure 2-4 SEM image of roughness on machined PMMA [3].....	29
Figure 2-5 Figure 1-1 SEM images of bulging on walls of PMMA copied from Cheng et. al. a.) Cast PMMA substrate without annealing. b.) Cast PMMA substrate after annealing. c.) Extruded PMMA substrate without annealing [29, 30]......	30
Figure 2-6 PDMS	32
Figure 2-7 Microscope glass slides	33
Figure 2-8 SEM software.....	34
Figure 2-9 SEM machine	34
Figure 2-10 Optical Profilometer	35
Figure 2-11 Muse laser setup	36
Figure 2-12 Profiler image of sample when power is at 10%, speed 10 mm/sec, current 20mA, pass1	38
Figure 2-13 3D Profiler image of sample when power is at 10%, speed 10, current 20, pass1	38
Figure 2-14 width and depth of the cut by varying power at speed 10mm/sec, current 20, single pass at focal length	39
Figure 2-15 Varying Speed Glass By taking rest of parameters as constant value (speed vary, Pass 1, current 20mA, power 4.5W).....	40
Figure 2-16 Profiler image of glass when speed is 15mm/sec,Pass 1, current 20mA, power 4.5W.....	41
Figure 2-17 3D Profiler image of glass when speed is 15mm/sec,Pass 1, current 20mA, power 4.5W.....	41
Figure 2-19 Varying Focal length Glass when power is 9 Watts, current 20mA, speed 10mm/sec, single pass	43
Figure 2-20 Profiler image of Glass placed at 0.30 Cm distance from tip of the lens when power is 9 Watts, current 20mA, speed 10mm/sec, single pass	43
Figure 2-21 3 D Profiler image of Glass placed at 0.30 Cm distance from tip of the lens when power is 9 Watts, current 20mA, speed 10mm/sec, single pass	44
Figure 2-22 Date obtained from profiler when Glass is placed at 0.30 Cm distance from tip of the lens power is 9 Watts, current 20mA, speed 10mm/sec, single pass	44

Figure 2-23 Varying Passes for Glass when power 4.5W, current 20 mA, Speed 10mm/sec at focal length	45
Figure 2-24 Single pass when current is 4.5mA, power=20W,speed10 at focal point	45
Figure 2-25 two pass when current is 4.5mA, power=20W,speed10 at focal point	46
Figure 2-26 Three pass when current is 4.5mA, power=20W,speed10 at focal point	46
Figure 2-27 four pass when current is 4.5mA, power=20W,speed10 at focal point	46
Figure 2-28 Control of shape of cut by varying passes	47
Figure 2-29 Surface roughness Images at speed 25mm/sec	49
Figure 2-30 Optical Profilometer image at speed 25mm/sec	50
Figure 2-31 Roughness data obtained from Profilometer at speed 25mm/sec	50
Figure 2-32 Varying power at Current=20mA, Speed=10mm/sec, Pass 1 at focal length	52
Figure 2-33 10% of total power speed 10 pass 1 current 20 at focal length	52
Figure 2-34 Varying focal length at speed 10mm/sec, current 20mA, power 20%	53
Figure 2-35 Speed 10mm/sec, Power 20% of total power, pass 1 current 20mA focal distance between lens and substrate 0.30 Cm	54
Figure 2-36 PMMA at speed 5, power 10%, current 20, single pass at focal length	55
Figure 2-37 Varying Speed at 10% of total power, current (20mA) and passes (1) at focal length	56
Figure 2-38 Varying Pass at 10% of total power i.e. 4.5W, current 20 mA, speed 10mm/sec	56
Figure 2-39 Controlling of shape by increasing pass	57
Figure 2-41 PDMS varying power at (Speed 10mm/sec, current 20mA, Pass 1	59
Figure 2-42 PDMS at 30% of total power, current 20, speed 10, pass 1 at focal length...	59
Figure 2-43 Variation of focal distance at at speed 10mm/sec, current 20mA, power 20%	60
Figure 2-44 PDMS vary in speed at current 20 mA, power 5Watts (10% of total power), pass 1	61
Figure 2-45 SEM image of PDMS at speed 5, power 10%, pass 1, current 20mA	62
Figure 2-46 PDMS at 10% power, current 20, speed 10mm/sec	62
Figure 2-47 Control of shape of cut	63
Figure 2-49 Roughness data obtained from profilometer at speed 25mm/sec	64
Figure 2-50 3D profilometer image	65
Figure 2-51 Comparison of PDMS, PMMA and Glass by varying power	66

Figure 2-52 Comparison of PDMS, GLASS, PMMA in terms of depth by varying power	67
Figure 2-53 Comparison of PMMA, PDMS, and GLASS by varying speed in terms of width	68
Figure 2-54 Comparison of PMMA, PDMS, GLASS by varying speed in terms of depth	69
Figure 2-55 Comparisons of PMMA, PDMS and Glass by varying focal length in terms of depth	70
Figure 2-56 Comparisons of PMMA, PDMS, GLASS by varying focal length in terms of width	71
Figure 2-57 Comparison of PMMA, PDMS, Glass at various Pass in terms of width of cut	72
Figure 2-58 Comparison of PMMA, PDMS, GLASS at various Pass in terms of Depth of cut	73
Figures 3-1 Titanium Round samples	79
Figure 3-2 Titanium Rods	79
Figure 3-3 Titanium Flat samples	80

Table of contents:

Table 2-1 Range of wavelength of light[16].....	24
Table 2-2 Surface roughness data	48
Table 2-3 Roughness data for PDMS	65

Abstract

LASER (Light Amplification by Stimulated Emission of Radiation) has many applications in engineering, biology, biomedical etc. Recent years, laser micromachining has become a promising technology for mass production of surface texturing on various polymeric substrates and metals. However, excessive roughness of channel surface, lack of control of process parameters and no uniformity of channel geometry are the ongoing challenges. The goal of the study is to determine the effect of laser system parameters on the surface of different kinds of polymers (PMMA, PDMS and Glass) as well as metals (Titanium).

There are two specific objectives in this study. The first objective was to determine the effect of laser parameters on different kinds of polymers. A commercial MUSE laser system was used for machining three widely used microfluidic substrates to create microfluidic channels, which consists of a 45W laser tube with three degree of freedom (lateral, longitudinal and vertical). Four laser system parameters - speed, power, focal distance and number of passes are varied to fabricate straight microchannel on glass, PDMS and PMMA. The results show that higher speed produces lower depth while higher laser power produces deeper channel regardless of the substrate materials. The out-of-focus laser cut produces wider but shallower channel. However, for same speed and power, PDMS channel had the roughest surface and PMMA had smoother surface. In PMMA, a uniform and wider channel was produced with the number of passes, which when increased can control the bulging phenomenon. This comprehensive experimental investigation can provide guidance for the substrate material-based mass production of microchannels.

The second objective was to investigate the effect of nitriding on a laser textured titanium surface to improve its optical properties for application in solar thermo photovoltaic. Nitriding of titanium alloy samples were carried out in plasma nitriding furnace after laser engraving. Full spectrum high power laser machine was used to make grooves on titanium alloy. The study found that laser textured nitride titanium has better surface properties and increased optical properties when compared to those of non-nitride titanium. For better understanding of the TiN on Ti , X-ray photoelectron spectroscopy(XPS) was carried out before and after plasma treatment. XPS analysis found nitriding has positive influence on the surface characteristics. Nitriding makes the laser grooved Ti surface more reflective compared to those of non-nitriding Ti surface.

CHAPTER 1

INTRODUCTION

1.1 Summary

Laser (Light Amplification by Stimulated Emission of Radiation) has numerous applications in engineering, biomedical, biology etc. The goal of this study is to know how the lasers parameters are going to effect different polymers as well as metals. In order to know the effect of polymers, a microfluidic channel is developed using different laser parameters on three different materials as microfluidics has numerous advantages in capillary electrophoresis, DNA analysis, detection of cancer, separation and manipulation of cells etc. Materials used are Glass, PMMA (Polymethylmethacrylate), PDMS (Polydimethylsiloxane). Five Laser parameters are varied to evaluate the effect on materials such as Speed, Current, Power, Pass and change in focal length. Roughness, profile shape, length of the cut, width of the cut are evaluated. From the comparison it is found that PMMA has more depth of the cut, PDMS has more width of the cut as well as more surface roughness for a laser parameter set when compared to other materials. In order to know the effect of laser parameters on metal, laser micro textures are created on the titanium flat sample and the XPS analysis is carried out. Three sets of samples are prepared controlled, laser treated, laser plusTiN treated Ti (ITiN). All the titanium samples are well polished before treating with laser. Laser treated Ti samples are used to improve the efficiency of thermos photovoltaic cell.

1.2 Laser micromachining

Laser machining is the process of removing small amount of material from substrate surface using focused laser beam. Most commonly used materials are Polymers, Metals, Ceramics and composites. The following are the types of laser micromachining process

1. Direct writing

2. Mask projection

1.2.1 Applications of laser Micromachining:

The following are the applications of laser micromachining:

1. Used in drilling micro holes

2. They are used in manufacture of micro channels and micro holes in integrated chips and microchips

1.2.1.1 Advantages

Advantages of Micromachining process includes:

1. Easily capable of being automated

2. Straight forward process monitoring

3. Minor amount of heat-affected zone

4. Machining free from burr and bulging

5. More flexibility while designing of microstructures

6. Better machining speed

7. Better precision

Disadvantages:

1. Expensive

2. Highly skilled people are needed operate micro machining systems.

3. limitations of material

1.3 Hypothesis

Two hypothesis are tested in this thesis. The first hypothesis of this study is the combination of laser parameters and material properties that can produce smooth functional microchannel. A functional microchannel has controlled channel profile and smoother surface finish. The second is to find the effect of nitriding on a laser textured titanium surface to improve its optical properties for application in solar thermo photovoltaic.

1.4 Thesis Statement and objectives

Two independent studies are conducted to test the above hypothesis. To test first hypothesis following objectives are pursued.

Objective 1:

Determine the effect of laser parameters scanning speed, current, passes, focal length, and power on glass substrate. The effects are evaluated by measuring depth, profile shape, width of the cut using SEM and Optical 3D profilometer.

Objective 2:

Determine the effect of laser parameters scanning speed, current, passes, focal length, and power on PMMA substrate. The effects are evaluated by measuring depth, profile shape, width of the cut using SEM and Optical 3D profilometer.

Objective 3:

Determine the effect of laser parameters scanning speed, current, passes, focal length, and power on PDMS substrate. The effects are evaluated by measuring depth, profile shape, width of the cut using SEM and Optical 3D profilometer.

Objective 4:

Comparison of PMMA, PDMS, and Glass in terms of depth and width of the cut

A rigorous analysis of the results for objectives are conducted and a recommendation to optimum laser parameters on substrate material is determined.

The second part of thesis shows how the laser parameters are going to effect titanium metal:

Goal of this study is to measure the impact of laser assisted microtextures on absorption of nitrogen in titanium to create titanium nitride coating on Ti and to evaluate optical properties for application of solar thermo photovoltaic cell.

1.4.1 Objectives

To examine or to analyse

- 1.The effects of laser assisted groove topography on physical responses of Titanium
- 2.The effects of laser assisted groove topography on Attachment of nitrogen on Ti surface

1.5 Organization of thesis

The first chapter provides brief overview of study of thesis objectives. Chapter 2 mainly concentrates on microfluidic substrate polymers. It provides how the laser parameters are going to effect PMMA, PDMS and Glass. A microfluidic channel is developed using different laser parameters and the depth of the cut, width of the cut, control of shape of cut for PMMA, PDMS and Glass are evaluated. Roughness analysis, quality of microchannels are also discussed. for PDMS and Glass are carried out in chapter 2. Chapter 3 mainly concentrates on titanium metals. It says how the laser surface textures are going to effect titanium metal. It provides how the of laser assisted groove topography is going to respond on Attachment of nitrogen on Ti surface and without attachment of titanium. XPS analysis is done in chapter 3 for all the titanium samples. Chapter 4 is conclusion for laser affected polymers and titanium metal.

CHAPTER 2

Effect of Laser on Polymers

2.1 Summary

Microfluidic device usually consists of small number of channels, which are of micro in range. Microfluidic devices has numerous applications in engineering, biology, biomedical etc. They are used in capillary electrophoresis, flow cytometry, immunoassays, analysis of DNA, cell patterning etc. The goal of this thesis is to find co-relation between laser parameters and substrate materials.

2.1.1 Objectives:

The work here is presented in five main components.

1. Investigating or determining the co-relation between laser parameters and substrate materials. Substrate materials are Glass, PDMS, PMMA
2. Laser parameters are spot size, power, speed
3. Investigating or determining the surface properties (roughness) of the materials using Optical Profilometer and SEM (Scanning Electronic Microscopy)
4. Determining the length of the cut, Depth of the cut by varying one parameter at a time
5. Minimizing or reducing bulging, Cracks on walls

Micro or Nanofabrication techniques have been enormously developed over the past decade years[1]. These enable us to create various tiny and advanced structures for multiple applications. It has perceived a lot of things beyond imagination. As an example,

a full laboratory in micro scale can be equipped, so called Lab on Chip (LOC), soon. To develop a device, the fabrication technique, as well as system functionality, must be considered. Generally, microfluidics devices are designed and developed using Soft lithography, photolithography, and chemical etching techniques. However, these techniques are limited to Glass and Silica based materials. These microfabrication techniques are time consuming and require highly trained professionals[2]. Recently laser ablation has become most popular technique for fabrication of microfluidic devices. Laser ablation process uses an intensely focused beam to break down a material. Generally, UV (Ultraviolet) lasers and IR (Infrared) lasers are used for fabrication process. However, in UV lasers the laser beam is invisible and requires greater expertise to handle. UV lasers are more complex, larger and considerably more expensive. IR lasers on the other hand operates at the invisible wavelength of the light spectrum. IR laser on the other hand are cheap and not environmental friendly[3]. However laser ablation technique has some of the issues like bulge formation, Cracks on walls, irregular profile, more surface roughness etc. The goal of the study is to resolve these issues. The objectives are to determine the effect of laser parameters (scanning speed, current, passes, focal length, and power) on PDMS, PMMA and Glass substrates and compare them in terms of depth of the cut as well as width of the cut. The effects are evaluated by measuring depth, profile shape, width of the cut using SEM and Optical 3D profilometer.

2.2 Microfluidics and its applications:

Microfluidics is a science, which generally studies or deals with the behaviour of fluids through the micro-channels, and technology of engineering microminiaturized devices

consists of tunnels, and chambers through which fluids flow takes place. Microfluidics generally deals with small amount of fluids, down to femtoliters (fL). These unique features are the key for innovations and scientific experiments[4]. Because of the speed, small physical footprint, reduced reagent consumption and the efficiency of chemical separations, microfluidic devices is used in modern analytical laboratory[5]. Even Micro analytical system use these devices for protein separations and capillary electrophoresis[6]

2.2.1 Applications of microfluidics:

They possess numerous applications in chemistry, biology, biomedical and engineering some of them are:

Chemistry:

Microfluidic systems or devices are also used in some of the procedures such as isoelectric focusing, immunoassays, DNA analysis, cell patterning and separation and manipulation of cells.

Biology:

Research applications includes mainly in the study of transport of nanoparticle in blood and observation of chemical reaction kinetics.

Diagnosis and Biomedical applications:

Diagnostic includes cancer detection and pathogen detection.

Engineering applications:

Microfluidic devices used in measuring fluid viscosity, molecular diffusion coefficients, PH.

Biopharmaceutical applications:

Microfluidic systems has analytical uses in biopharmaceutical production mainly in monitoring and optimization of production of protein drugs as well as assays involving human cells.[7]

2.3 Conventional techniques and process:

Microfluidic devices can also be fabricated using conventional techniques. Some of them are Electron beam lithography, Optical projection lithography, Extreme UV lithography, photolithography, focused ion beam lithography etc.

Photolithography process usually consists of photo mask and photo resist. Photolithography process utilizes light coming from sun and is allowed to pass through geometric patterns from transparent mask to substrate. Photolithography process involves five steps. During the step one, the wafer has to be cleaned in order to remove any residue present on it and a barrier layer is applied on wafer. The second step involves spin coating the substrate at high speed with photoresist. Third steps involve evaporating the photoresist to remove solvents from it. Fourth step involves exposing the individual areas of photoresist to UV light through photomask. As the photoresist is exposed, it undergoes chemical reorganization. Positive photoresists, which are exposed to UV light, makes changes in the chemical structure of photoresist to which makes it highly soluble. Negative photoresists on the other hand when exposed to UV light, becomes polymerized

and hard to dissolve. The fifth step involves developing positive photo resist and negative photo resist. Positive photo resist involves disintegrating the areas of photoresist that are exposed to UV light by immersing the substrate in developer solution. . As a result, the photoresist will be patterned with the exact master image that was provided by the user. Negative photoresist involves dissolving the unexposed parts of photoresist in developer solution. As a result, the mask engaged for negative photoresist holds inverted reproduction of pattern to be transferred on to the wafer[8].

Bahadorimehr, B. Y. Majlis presented a paper on Glass-based Microfluidic Devices. He used Photoresist as Mask and obtained a depth of 150 μm by using a photoresist and wet etching process. Initially coating was made on the glass surface with photoresist AZ 5214, by spinning using spin-coater, followed by post baking there by immersing the glass substrate in an etchant using special concentrations of Hydrofluoric acid (HF), Ammonium Fluoride (NH_4F), Hydrochloric acid (HCL) and DI watering a magnetic stirring bath. From the results, they found that HF-based methods, has more rough surface, but addition of HCl, Buffered Oxide Etchant (BOE) and DI water provides better smooth surface.

Wet and dry etchings are the most as often as possible utilized technique for the manufacture of micro scale or Nano structures. There are a ton of formulas accessible for different materials[9].Wet etching includes chemical reaction between an etchant and a substrate to evacuate material and so as to make a specific structure, a masking process is certainly important to protect unwanted regions on the substrate[10]. On the other hand, dry etching utilizes chemical interaction or physical bombardment using plasma

innovation[11]. It is easy to control dry etching parameters when compared to wet etching process. It also produces less toxic material when compared to wet etching process[12]. Reactive ion etching (RIE), Plasma etching, and deep reactive ion etching (DRIE) are the major dry etching techniques. Dry drawing procedure likewise needs a masking process, for example, photolithography, which is for the most part utilized in semiconductor industries. Nanolithography is the fabrication technique for the structures normally under 100nm scale. There are a few nanolithography techniques. Soft lithography is the fabrication technique, utilizing a patterned or designed elastomer as a stamp, mold or mask[13]. In general, Soft lithography incorporates, molding (REM), micro contact printing (μ CP), capillaries micromolding (MIMIC), solvent assisted micro molding (SAMIN) and micro transfer molding (μ TM), and it can make the structures, extending from 30nm to 100 μ m[14].

However, conventional microfabrication technology has some issues some of them are high capital investment, Maintenance cost, Use of chemicals, requires more time etc. In order to avoid this, laser ablation technique came into existence. It is a promising technique for microfluidics.

2.4 Laser technology:

Laser machining usually uses to cut metals, drill a gap, for example, ink-stream printer spouts, and straightforwardly manufacture or fabricate small scale/Nano structures[15]. "LASER" represents Light Amplification by Stimulated Emission of Radiation. Light has distinctive wavelength extending from 1nm to 1000 μ m as appeared

in Figure 2.2. Behind DUV, the x-beam has very short wavelength (0.01nm to 10nm), which is considered as the source for the X-beam lithography. Laser can be grouped with the sort of laser sources – strong, gas and semiconductor.

200nm 400nm 700nm 10μm

DUV	UV	VISIBLE RAYS	NIR	FIR
-----	----	-----------------	-----	-----

Table 2-1 Range of wavelength of light[16]

DUV: Deep Ultraviolet

UV: Ultraviolet

NIR: Near Infrared

FIR: Far Infrared

The gas laser can be grouped by the wavelength. Excimer laser has the wavelength running from 157nm to 351nm. Then again, ND: YAG has 266nm to 1.06μm wavelength and CO2 has 10.6μm wavelength. All in all, shorter wavelength gives the higher goals to make structures. Besides, the short wavelength laser uses laser removal rather than warm impact to expel material. Then again, longer wavelength laser, including ND: YAG and CO2 utilize a warm impact to make structures. Laser machining has several advantages when compared to other techniques some of them are Few processing step, capable of serial and batch-mode production processing, high flexibility, no major investment required, applicable to a wide range of materials such as polymers, glasses and metals[16]

2.4.1.1 Applications of CO₂ Lasers:

CO₂ lasers highlight numerous qualities, which make them perfect to fit modern applications. Some of them are

1. Inexpensive
2. More efficiency
3. Wide possible variation in output of the power
4. More lifetime[16]

Laser ablation technique is the process of removing top most layer of the material from solid substrate by irradiating it with continuous focused laser beam[17].

2.4.2 Applications of Laser Ablation Technique:

- a) Laser ablation is used in medical field including, general surgery, neurosurgery, ophthalmology, ENT, oral and dentistry[18]
- b) They are used in removing tumors and lesion.
- c) Used in soft-tissue surgeries[19]
- d) Used in automotive and aerospace industries
- e) Used laser machining and laser drilling
- f) Used in removing rust from iron objects
- g) Used to create plasma from the material surface[19]

Recently it has been used for micro and nanofabrication, because of less amount of heat deposition on the targeted surface, high resolution capability, and high level of flexibility[20]. This technique has several advantages as it involves less cost, faster

processing, more efficient[21], doesn't require clean room, involves less residual waste and moreover environmentally friendly[22]. Some of the disadvantages include irregular profile shape, more surface roughness, and bulge formation across walls.

Besides advantages and disadvantages laser ablation techniques has some ongoing challenges some of them are excessive roughness of channel surface, lack of control of process parameters, cracks on walls and no uniformity of channel geometry are the ongoing challenges. Figure 2-1 shows the cracks on the walls of PMMA substrate. Figure 2-2 shows bulge formation on walls of PMMA channel after treated with laser.

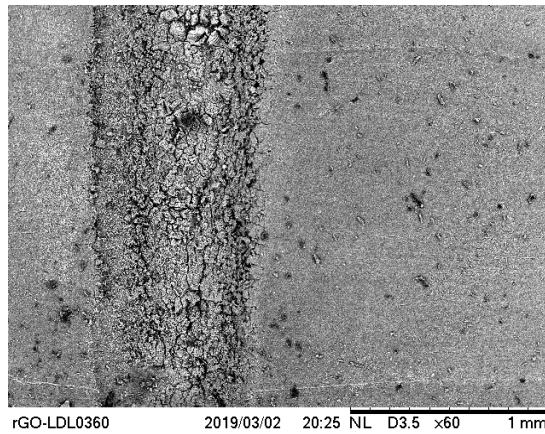


Figure 2-1 Crack on walls of PMMA substrate after treating with laser

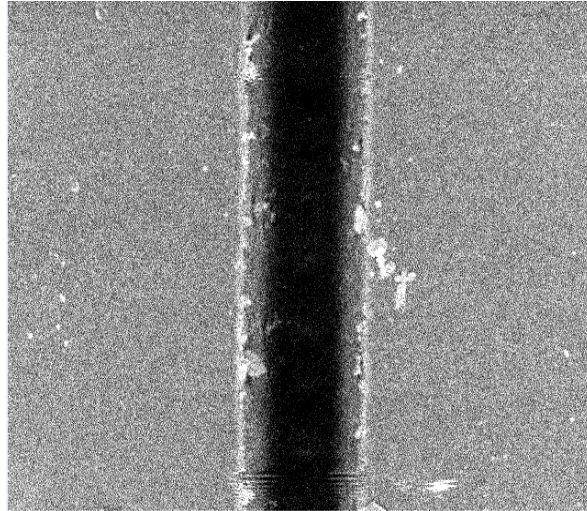


Figure 2-2 Bulge formation on walls of PMMA when treated with laser

Various materials were used for fabrication of microfluidics. Tao Wang presented a paper on Fabricating Microstructures on Glass using Glass Moulding technique, where he reduced the surface roughness R_a , as small as 10 nm[22]. Muhammad Imran, presented a paper on Fabrication of PMMA using CO₂ laser. By increasing the number of passes he controlled the shape of cut[23]. In order to understand how the laser parameters are going to effect PDMS, PMMA and Glass, this paper shows the comparison of PMMA, PDMS and Glass in terms of depth as well as width of the cut.

2.5 Laser fabrication of microfluidics:

People have been moving in direction of extending the utilization of lasers into the domain of microfluidics. The utilization of lasers in microfluidics can be separated dependent upon the what type of laser used. Two types of laser are used in microfluidics depending upon the application, Pulsed UV light lasers, or Continuous infrared (IR) light lasers. Use of high energy light in UV lasers, induces breakdown of targeted material in

short pulses. This sort of laser is utilized to add unmoldable features to the microchannel [24-26]. UV lasers are also used for direct micromachining of microchannel in PMMA[3]. However, UV lasers have wider range of applications, their repetition rate and cost limits their usage. On the other hand, IR lasers in the form of CO₂ laser had many applications in industrial areas[27]. They are commercially available at cheap price when compared to those of UV lasers. They have several advantages in speed, low cost and more flexible.

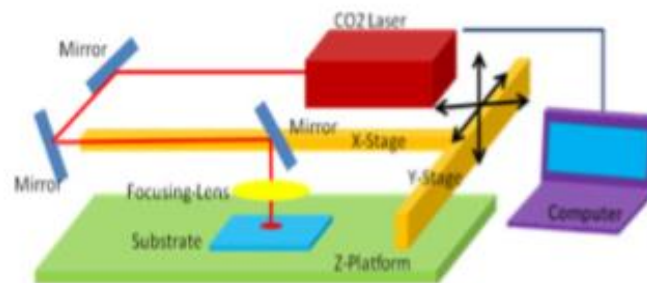


Fig. 1 Configuration of direct-write laser machining system

Figure 2-3 direct write laser machining system configuration [28]

Cheng et. al.[29] used CO₂ laser on PMMA substrate and found that roughness can be reduced from 5-10 μ m to 2-3 μ m on application of thermal annealing process. Figure 2-3 shows the direct write laser machining configuration system. Besides roughness problem, they investigated bulging distortion on channel rim. From the results, they found that two types of PMMA substrate are present cast and extruded. This study found that extruded PMMA had less roughness and more bulges on the other Cast PMMA has more roughness and less bulges across channel rim. Henning Klank[30] used CO₂-laser

micromachining as well as back-end processing in order to produce PMMA-based microfluidic systems. This paper primarily focus on PMMA substrate. Additionally polymers, which are resistant to thermal decomposition are used, as the material removal in CO₂ laser is purely thermal. PMMA breaks down to volatile products leaving clean structures behind. However, some of concerns were discovered. The first was bulge formation across the walls of targeted surface that is due to solidification of ejected material from solid surface. The second was the roughness i.e. about 1-2um, which can results in limiting the use in applications[29]. Fig 2-4 shows SEM images of roughness on machined PMMA.

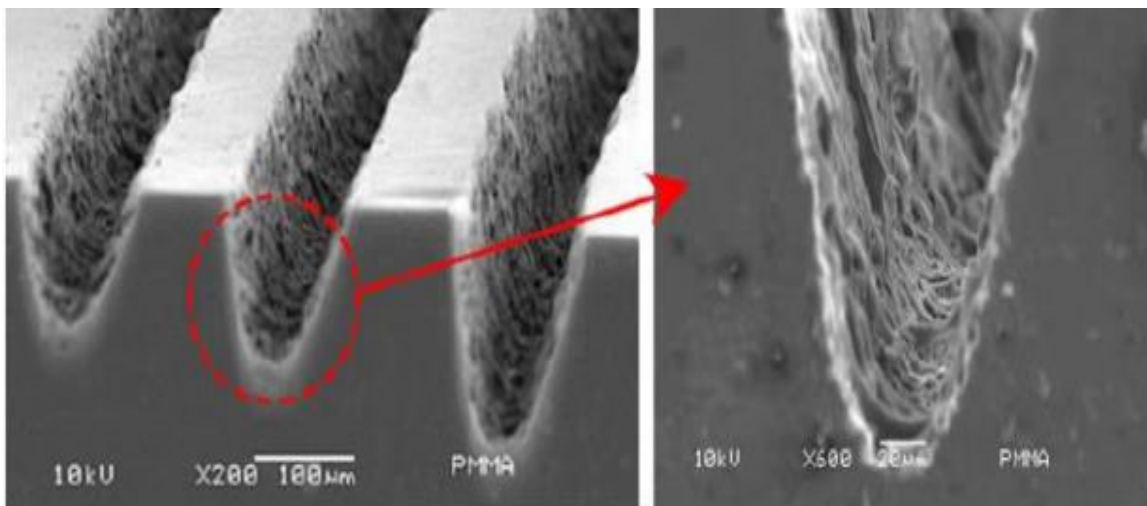


Figure 2-4 SEM image of roughness on machined PMMA [3].

Ting-fu Hong[29] proposed a paper on Rapid PMMA substrate using CO₂ laser. Figure 2-5 shows SEM images of bulging PMMA. The study primarily focuses on PMMA

substrate. The results show that a smoother microchannel surface is obtained by using unfocused laser beam. He obtained roughness of about $0.004\mu\text{m}$ using unfocused laser without the need of annealing (post processing process).

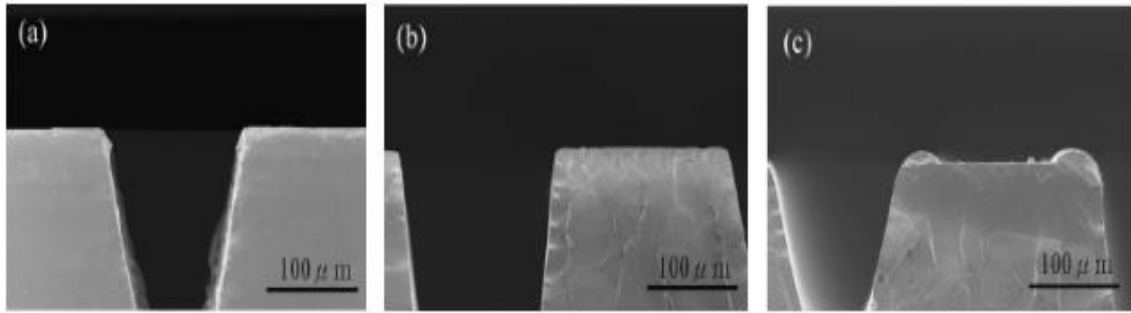


Figure 2-5 SEM images of bulging on walls of PMMA copied from Cheng et. al.. a.) Cast PMMA substrate without annealing. b.) Cast PMMA substrate after annealing. c.) Extruded PMMA substrate without annealing[29, 30].

However, Surface roughness, bulge formation, cracks on walls, Irregular profile shape are the ongoing challenges for the smooth flow of liquid in microfluidic devices.

2.6 Materials and Methods:

2.6.1 Materials:

Fabrication of microfluidic device is carried out on PMMA, PDMS and Glass substrate.

2.6.1.1 PDMS:

Materials used to prepare PDMS:

- 1.Silicone elastomer curing agent
- 2.Silicone elastomer base
- 3.Stirring tool
- 4.Plastic Weighing dish
- 5.Digital scale
- 6.Glass plate
- 7.Desiccator
- 8.Oven
- 9.Indoor mounting tape
- 10.knife
- 11.Compressed air
- 12.Ruler
- 13.Cutting board
- 14.Chip of desired size
- 15.Rubbing alcohol
- 16.Paper towel

Preparation of PDMS:

PDMS is a silicon-based organic polymer. In microfluidic chips, PDMS is used as a flexible membrane between control and Flow layer. It allows the chip to seal in the

desiccator and allows the actuation in flow manipulating valves. Valves required either positive or negative pressure to open and close. To allow proper evacuation you have to use the appropriate thickness of PDMS.

Mix Elastomer base and curing agent in 1:10 ratio for 10 minutes and put it inside desiccator using a tray. This desiccator removes the air bubbles typically. After 5 minutes open and close valves suddenly to pop the bubbles in the mixture. Repeat this until all bubbles have popped. Remove pressure in the desiccator and remove the tray. Now pour the elastomer mixture on a glass plate of the desired shape. If the bubbles form while flowing, use pipette tip or another sharp object to pop them off and leave the mixture of 1 hour. Reheat the oven to 100 C and place the tray inside for 1 hour. After that remove PDMS from oven and cool it for at least 45 min. Figure 2-6 shows PDMS.



Figure 2-6 PDMS

2.6.1.2 PMMA:

PMMA sheets are thermoplastic as well as transparent. They are used as lightweight alternative to glass. PMMA is available in the market in the form of big sheets. The sheets are cut down into 50x50 mm using cutting machine. Once the sheets are cut down, these pieces are used for fabrication of microfluidic device.

2.6.1.3 Glass:

Glass is another material early used for fabrication of microfluidic devices. It has several advantages in thermal conductivity, surface stability, and solvent compatibility. In this paper, a fine ground edged 75*25*1mm microscopic glass slide is used for fabrication.

Fig 2-7 shows microscopic glass.



Figure 2-7 Microscope glass slides

2.6.2 Scanning Electron Microscope (SEM)

Scanning Electron Microscope (Hitachi, Tokyo, Japan) was used to measure the width as well as depth of the channel created during laser ablation process. Images were taken under 5 KV and 10 KV accelerating voltages. Figure 2-8 and Figure 2-9 shows SEM software and hardware.

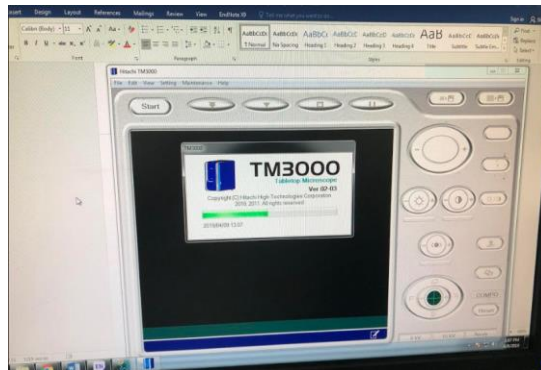


Figure 2-8 SEM software



Figure 2-9 SEM machine

2.6.3 Optical Profilometer

This thesis mainly uses 3D optical Profilometer to find the roughness as well as bulging values of microfluidic channels. Profilm3D consists of white light interferometry (WLI) which is used to measure surface profile as well as roughness down to $0.05\ \mu\text{m}$. It also consists of PSI option takes the minimum vertical estimate size down to $0.001\ \mu\text{m}$ [30]. Figure 2-10 shows the optical profilometer. This equipment should be free from noise and vibrations. Fig 2-10 shows Optical Profilometer.

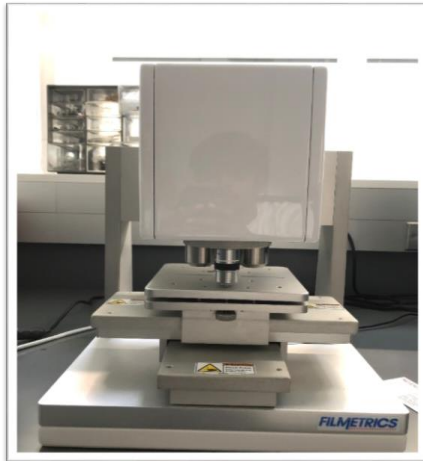


Figure 2-10 Optical Profilometer

2.7 Experimental setup and Preparation:

2.7.1 Muse laser setup:

In this process, a microscopic slide of $75*25*1\text{mm}$, PDMS and PMMA are fabricated using muse full spectrum laser machine. Muse laser machine has a total power of 45 watts, which usually consists of the Exhaust system, cooling system, and air compressor. The focal lens can move in x- direction, y-direction, and z- direction. The

laser beam coming out from the tube falls on mirror 1 are reflected to mirror two and falls on mirror 3. The laser beam, which is falling on mirror 3, is directed to the object. The Pattern, which is used for fabrication of microfluidic device, is drawn on AutoCAD software and finally exported to muse software (Retina Engrave). Muse software uses run perimeter command to find the perimeter where the laser is going to fire. Once the perimeter is found, the substrate is placed inside the perimeter. Hit on run job command, which makes the laser to fire in that particular perimeter. It is essential that your laser is tested and adjusted (if needed) for proper use before you start your first job. Proper alignment leads to best results. The depth as well as length of the cut is measured using Profilm 3D at various focal length, speed, power and passes in order to know the effect of different parameters on particular object. Figure 2-11 shows muse laser setup

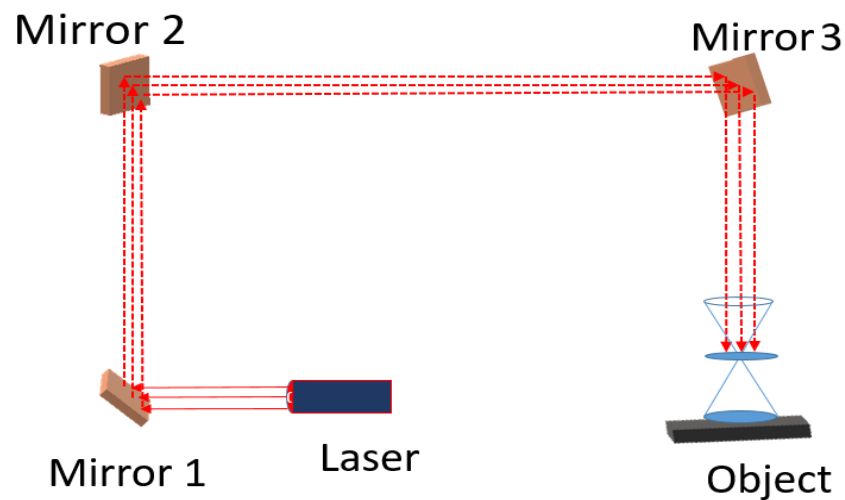


Figure 2-11 Muse laser setup

2.8 Results

2.8.1 GLASS:

Glass is one of the most commonly used material in fabrication of microfluidics. During this process, glass is heated up above evaporation temperature using CO₂ radiation. Due to high heat, top most laser of glass surface is ablated. As a result a microfluidic channel is developed. In this process, a glass substrate is placed under lens and microfluidic channel is developed by taking one parameter at a time and by putting the rest of parameters as constant. Laser parameters are Speed, current, power, focal length and pass. Three trials are conducted to have consistent results.

2.8.1.1 Varying Power:

To find the effect of laser power on microscopic glass substrate, the glass slide is placed exactly at focal distance i.e. 0.68 cm from lens. The laser tube has the total power of 45 watts. The glass is cut at 10% of total power, 20% of total power, 30% of total power and 40% of total power by putting the rest of parameters to constant value (speed 10mm/sec, single pass, current 20mA). Three trials are conducted for consistent results. The depth and length of each cut are determined by using 3D Profilometer. Figure 2-12 represents profiler image when the glass is cut with 10% of total power by taking the rest of parameter values speed 10mm/sec, current 20mA, single pass to a constant value. The results obtained from profilometer are plotted in excel sheet. Fig 2-14 represents length and depth of the cut with vary in power. From the plot, it is clear that the depth and length of the cut on glass increases linearly with increase in percentage of total power.

This is because increase in percentage of total power increases the amount of heat used to ablate the surface as a result, the depth as well as length of cut increases. Figure 2-13 and 2-14 shows the profiler image when power is 4.5W, speed 10 mm/sec, current 20mA and single pass. Figure 2-15 shows the width and depth of the cut by varying power at speed 10mm/sec, current 20, single pass at focal length.

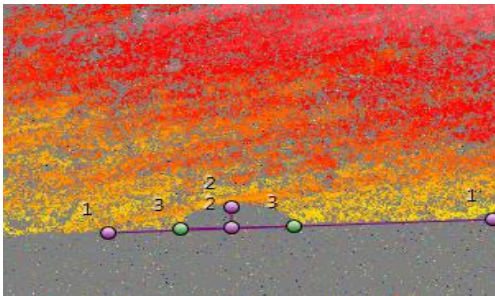


Figure 2-12 Profiler image of sample when power is at 10%, speed 10 mm/sec, current 20mA, pass1

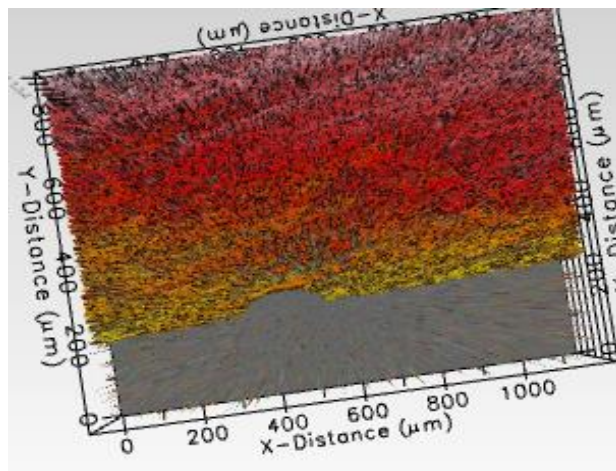


Figure 2-13 3D Profiler image of sample when power is at 10%, speed 10, current 20, pass1

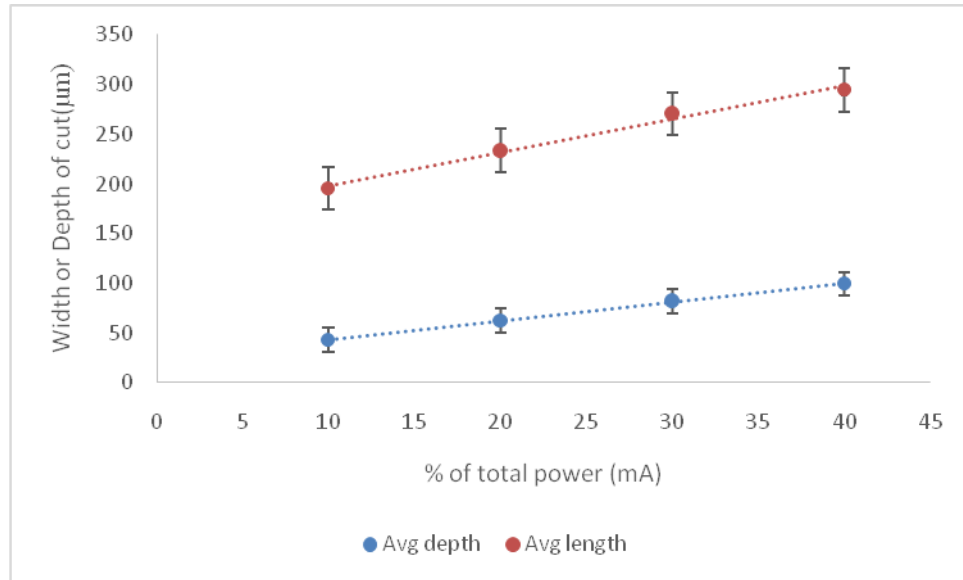


Figure 2-14 width and depth of the cut by varying power at speed 10mm/sec, current 20, single pass at focal length

2.8.1.2 Varying Speed:

During laser machining, three tests have been conducted on varying speed in order to have consistent results. Speed of the laser machine directly defines the exposure time of substrate[31]. Lesser the speed more will be the heat applied on the substrate, which leads to increase in depth. Speed is one of the most crucial parameters in laser machine. By varying the speed, the length of the cut, as well as depth, is varied. In this process, the laser beam is directed on the top of the microscopic glass at three different trails at different speed. In order to find the effect of speed, the laser power (10% of total power), current (20mA) and passes (1) are set to fixed value and the speed is varied at 5 mm/sec, 10mm/sec, 15mm/sec, 20 mm/sec, 25 mm/sec. The depth and length of the cut are determined using 3D Profilometer. Fig 2-17 and 2-18 shows profiler image of glass when

speed is 15mm/sec, Pass 1, current 20mA, power 4.5W. From figure 2-16 the depth of the cut as well as length increases with decrease in speed this is because the total amount of heat imparted on the material is less. As the speed is decreased, more amount of heat is imparted on the material, which leads to more length as well as depth of cut. Figure 2-16 shows varying Speed Glass By taking rest of parameters as constant (Pass 1, current 20mA, power 4.5W).

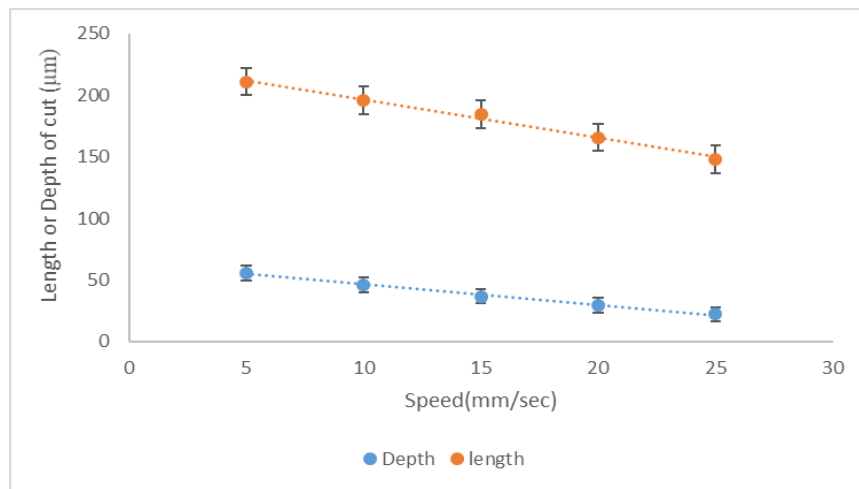


Figure 2-15 Varying Speed Glass By taking rest of parameters as constant value (speed vary, Pass 1, current 20mA, power 4.5W)

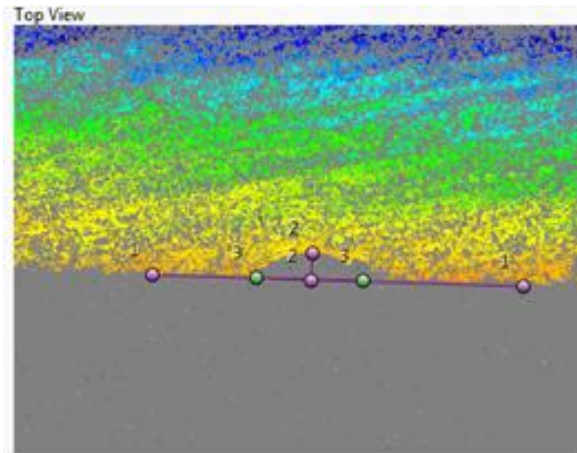


Figure 2-16 Profiler image of glass when speed is 15mm/sec,Pass 1, current 20mA,
power 4.5W

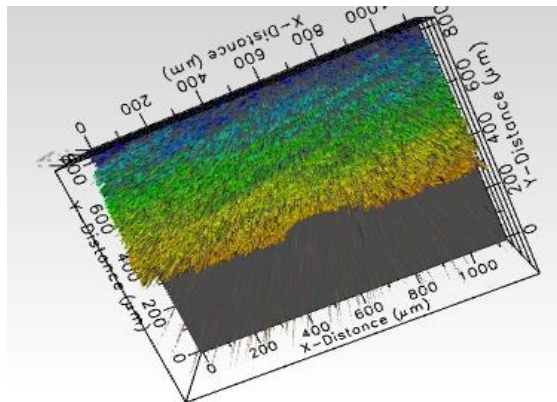


Figure 2-17 3D Profiler image of glass when speed is 15mm/sec,Pass 1, current 20mA,
power 4.5W

2.8.1.3 Varying focal length:

A beam is said to be focused when an object is placed exactly at focal distance from focal lens. When the substrate is placed at focal length, the spot size will be minimum as the beam converges to minimum radius value. The spot size increases by either increasing or decreasing the distance between focal lens and substrate other than focal distance. As a result, by adjusting the distance between substrate and focal lens, spot size can be controlled. It is important for an object or material to place it exactly at focal distance in order to have a fine cut. As a result, as the distance between the object and lens increases the spot size increases considerably the length of the cut increases there by reducing the depth. In order to know how the focal length is going to effect the microscopic glass, now the laser beam is directed on the top of glass slide at different focal length (0.3cm, 0.68cm, 1.06cm) by keeping the rest of parameters like speed(10mm/sec), passes(1 pass), power(9Watts) and Current(20m A) at constant value. Three trails are conducted in order to have consistency results. The length of the cut as well as depth are determined by using 3D Profilometer. From the result fig 2-20 we can see that the depth is maximum at focal point and it decreases by increase or decrease in focal length whereas the length is minimum at focal point and increases with increase or decrease in focal distance. Figure 2-18 shows varying Focal length Glass when power is 9 Watts, current 20mA, speed 10mm/sec, single pass. Figure 2-21, 2-22, 2-23 shows Profiler image of Glass placed at 0.30 Cm distance from tip of the lens(power is 9 Watts, current 20mA, speed 10mm/sec, single pass)

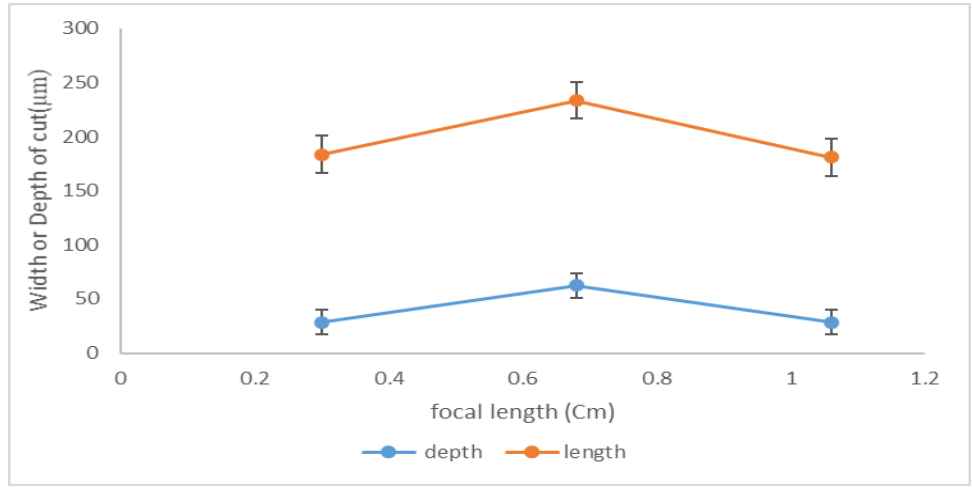


Figure 2-19 Varying Focal length Glass when power is 9 Watts, current 20mA, speed 10mm/sec, single pass

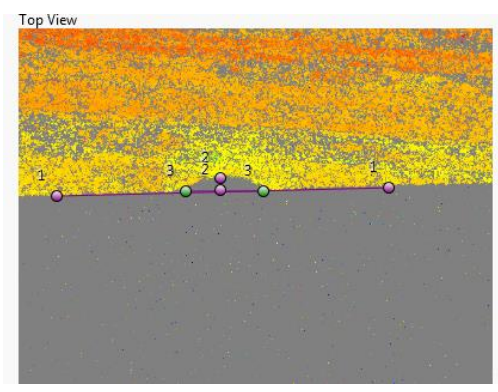


Figure 2-20 Profiler image of Glass placed at 0.30 Cm distance from tip of the lens when power is 9 Watts, current 20mA, speed 10mm/sec, single pass

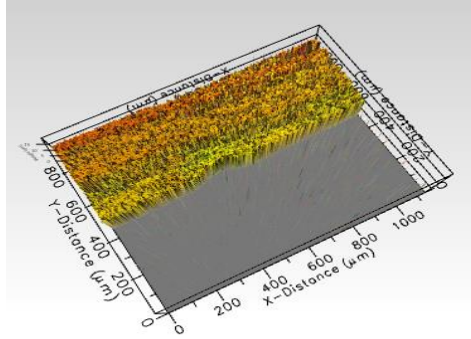


Figure 2-21 3 D Profiler image of Glass placed at 0.30 Cm distance from tip of the lens when power is 9 Watts, current 20mA, speed 10mm/sec, single pass

Delete	Name	Δx (μm)	Δy (μm)	Δz (μm)	Length (μm)
<input checked="" type="checkbox"/>	L1	789.2	19.83		789.5
<input checked="" type="checkbox"/>	L2	0	28.33		28.33
<input checked="" type="checkbox"/>	L3	184.5	0		184.5

Figure 2-22 Data obtained from profiler when Glass is placed at 0.30 Cm distance from tip of the lens power is 9 Watts, current 20mA, speed 10mm/sec, single pass

2.8.1.4 Varying Passes:

For the definition of deep micro channels, varying passes ablation process was repeated number of times. In order to find the true effect of passes on glass microfluidics, current, speed, power are kept to fixed value and the passes are varied at focal length. By varying the passes, the depth as well as length of the cut changes. The below figure 2-24 shows how the length of the cut as well as the depth is increasing by change in current. Figure 2-25, 2-26, 2-27 shows the profiler images of glass substrate

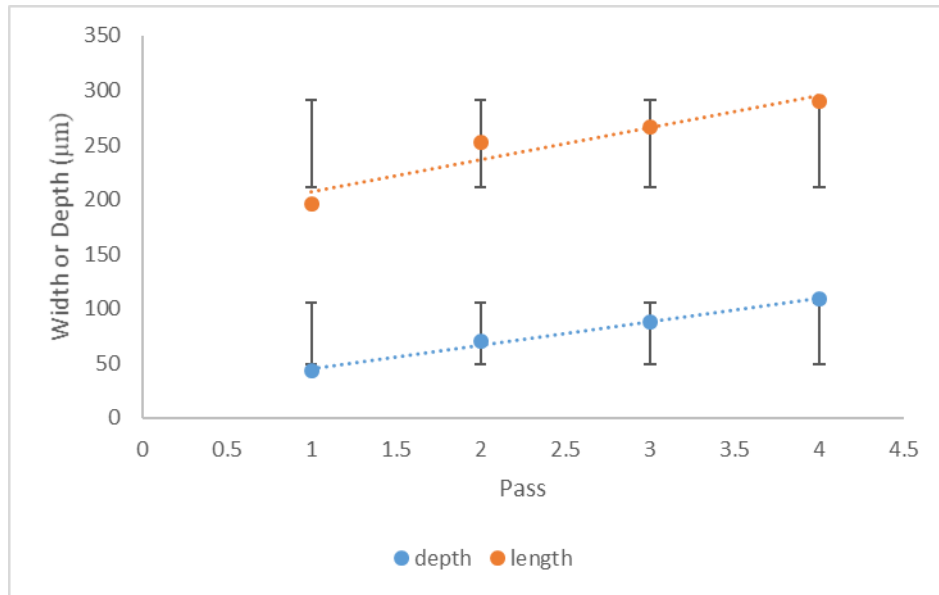


Figure 2-23 Varying Passes for Glass when power 4.5W, current 20 mA, Speed 10mm/sec at focal length

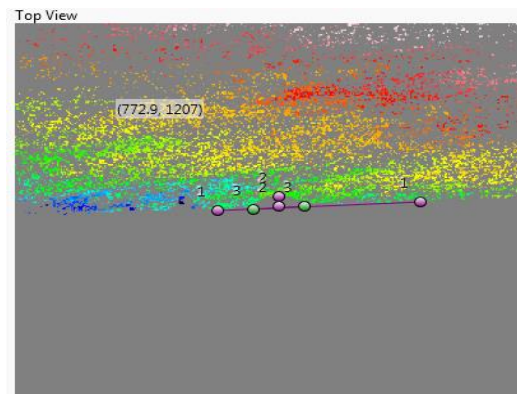


Figure 2-24 Single pass when current is 4.5mA, power=20W, speed10 at focal point

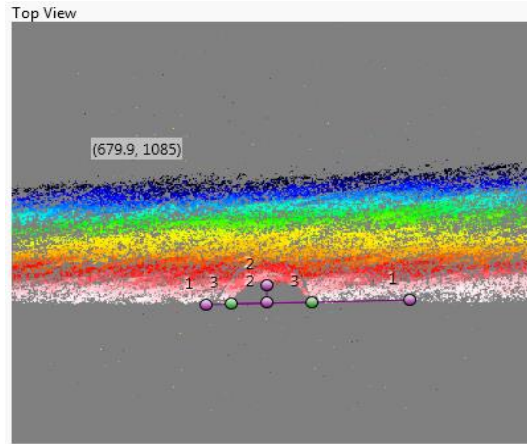


Figure 2-25 two pass when current is 4.5mA, power=20W, speed10 at focal point

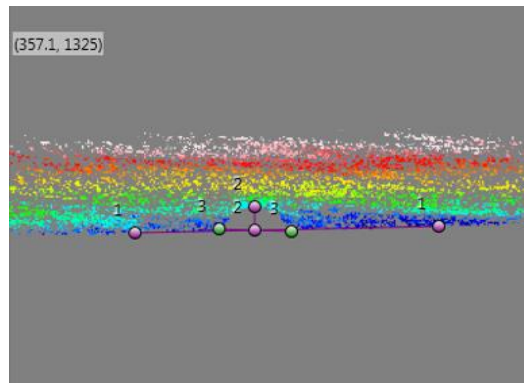


Figure 2-26 Three pass when current is 4.5mA, power=20W, speed10 at focal point

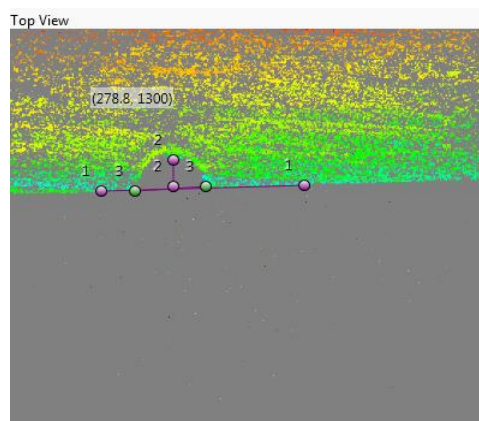


Figure 2-27 four pass when current is 4.5mA, power=20W, speed10 at focal point

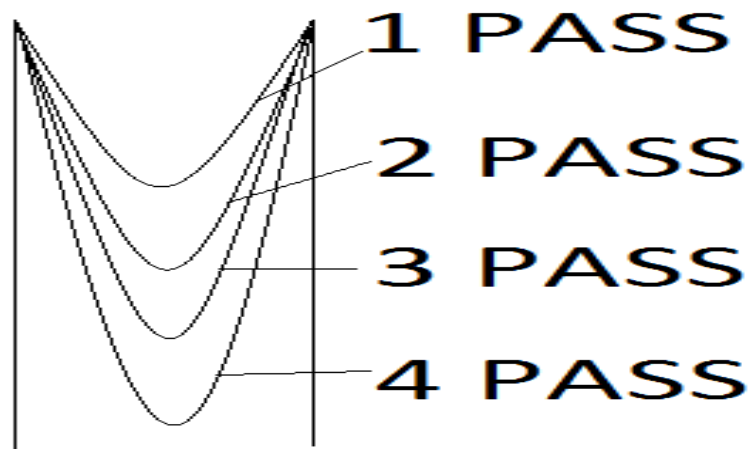


Figure 2-28 Control of shape of cut by varying passes

The above figure shows the profiler images of single pass, two pass, three pass and four pass. During single pass, the laser beam is directly going to hit the material. During two pass the laser beam is going to hit the material where the first beam was hit. During three pass the laser beam is going to hit where the earlier passes were hit. Due to this, the depth of the cut as well as the shape is changed and can be controlled by increasing number of passes. Figure 2-29 shows how the shape of the cut is varied.

2.8.1.5 Roughness Analysis:

Surface roughness of a microfluidic device is taken into consideration for the flow of liquid inside the microchannel from one end to other end. Microchannel with less surface roughness leads to more flow of liquid where as channel with more roughness leads to less flow of liquid. For the roughness analysis we used the microchannels that are prepared by varying speed and by taking the rest of parameters as constant. The surface

roughness analysis is carried out using optical 3- D Profilometer. Figure 2-30 and 2-31 represents surface images taken using optical profilometer. Figure 2-32 represents roughness data. The average roughness (Ra, μm) was taken as the mean of three (average of peaks and valleys of a surface) values measured in three different positions. Sa (Arithmetical Mean Height) represents the absolute value, the difference in the height of each point compared to the arithmetical mean of the microchannel surface. This parameter is used to evaluate surface roughness. Sq here represents the root mean square value of ordinate values within the definition area. Sq is equivalent to the standard deviation of heights. Table 2-2 shows the roughness data of varying Speed by taking rest of parameters as a constant value (Speed= Varied, Current = 20 mA, Pass 1, Power = 10 % of total power = 4.5 Watts at focal length

Table 2-2 Surface roughness data

Varying Speed	2.8.2 Sa (Arithmetical Mean Height)	Sq (Root Mean Square Height)
Speed 5mm/sec	0.4518 μm	0.5721 μm
Speed 10mm/sec	0.4559 μm	0.5509 μm

Speed 15mm/sec	0.4417 μm	0.6479 μm
Speed 20 mm/sec	0.3179 μm	0.5888 μm
Speed 25 mm/sec	0.6339 μm	0.7483 μm

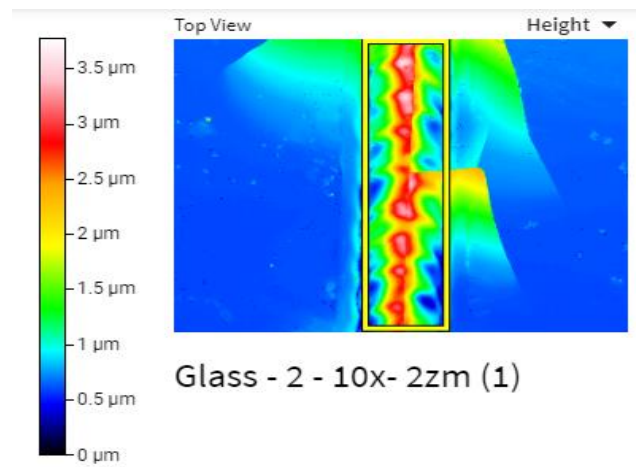


Figure 2-29 Surface roughness Images at speed 25mm/sec

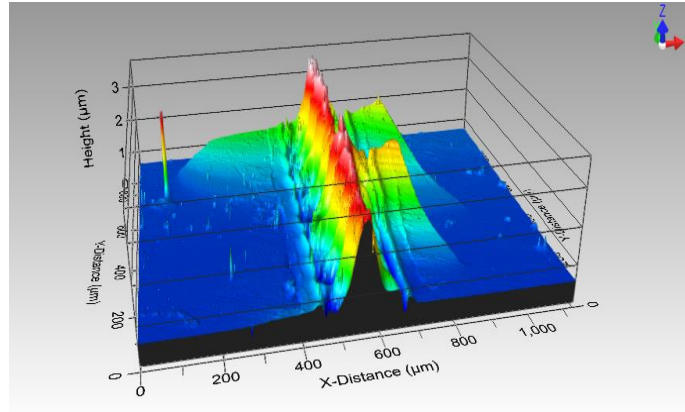


Figure 2-30 Optical Profilometer image at speed 25mm/sec

^ General			
Average	2.698	µm	Mean height
Minimum	0.6967	µm	Minimum height
Maximum	4.05	µm	Maximum height
Range	3.353	µm	Maximum - Minimum

^ ASME B46.1 3D			
Sp	1.352	µm	Peak height
Sv	2.001	µm	Valley depth
St	3.353	µm	Maximum peak to valley height
Sa	0.6339	µm	Arithmetic mean height
Sq	0.7483	µm	Root mean square height
Ssk	-0.4221		Skewness
Sku	2.221		Kurtosis

Figure 2-31 Roughness data obtained from Profilometer at speed 25mm/sec

2.8.3 PMMA:

PMMA (Poly methyl methacrylate) also known as acrylic is one of the most commonly used material in production of microfluidic device. PMMA is placed at different focal length and a microfluidic device is developed at various power, speed, Current and speed by putting the rest of parameters as constant. The cutting width of the substrate depends upon the aperture size as well as laser density. Even though the aperture size is same, the cutting width of the substrate increases with increase in number of laser pulses. The cutting depth of the substrate depends on laser density, aperture size, no of pulses per unit area as same as cutting depth.

2.8.3.1 Varying Power:

Fig 2-33 shows varying in percentage of total power. In this process a PMMA substrate is placed at focal length and the substrate is allowed to cut at different power i.e. 10 %, 20%, 30% and 40% by putting the rest of parameters to a fixed value. Laser parameters are set to speed=10mm/sec, single pass, current=20mA. The depth and width of the cut which are obtained by laser firing are measured using optical Profilometer as well as SEM microscope. Figure 2-34 represents SEM image at 10% of total power. The length and the depth of the cut obtained from SEM are plotted using Excel sheet. Figure 2-33 represents the results obtained from the plot. From the result it is clear that the length of the cut as well as depth increases linearly with increase in percentage of total power. This is because increase in percentage of total power increases the amount of heat used to ablated the surface as a result, the depth as well as length of cut increases.

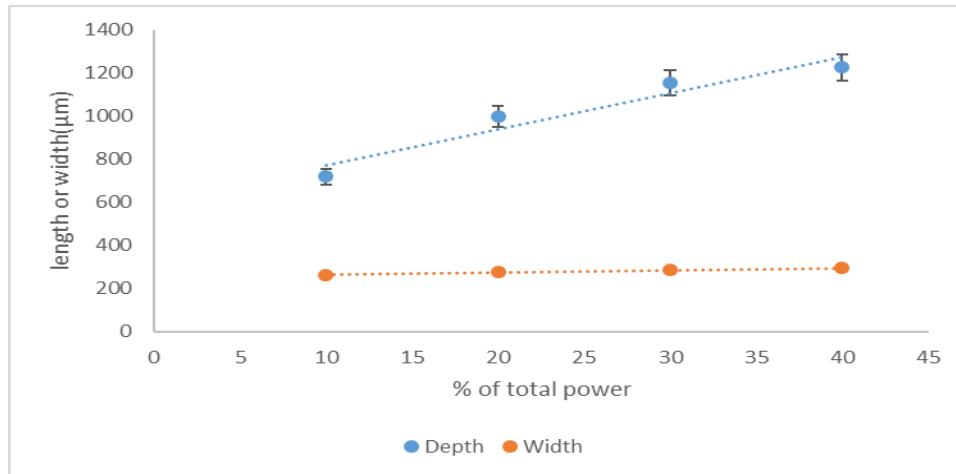


Figure 2-32 Varying power at Current=20mA, Speed=10mm/sec, Pass 1 at focal length

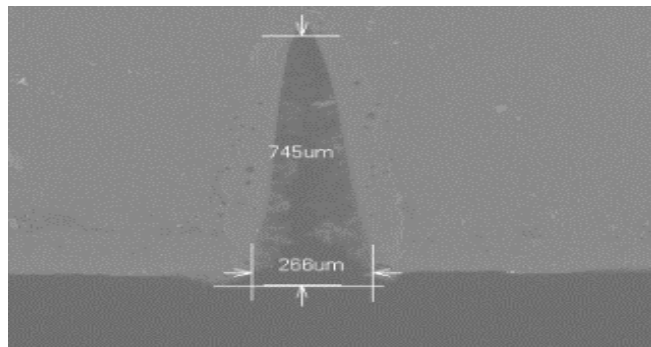


Figure 2-33 10% of total power speed 10 pass 1 current 20 at focal length

2.8.3.2 Varying focal length:

Laser beams are adjusted along x-axis and y-axis in order to create a microchannel using the laser ablation technique. Repeated ablation is done for deepening of channels along Z-axis. In order to know how the focal length of the laser machine is going to effect PMMA substrate, the focal lens of the laser machine is varied at different length and the graph is plotted. The width of the channel as well as depth are measured using Scanning Electronic Microscope as well as 3-D Profilometer. Figure 2-36 shows SEM image at Speed 10mm/sec, Power 20% of total power, pass 1, current 20mA and focal distance

between lens and substrate 0.30 Cm. In this process the focal length is varied at different points i.e. distance between the lens and PMMA substrate(0.68-0.38 = 0.30cm from Substrate), 0 , (0.68+0.38=1.06 cm) but putting the rest of parameters speed 10mm/sec, current 20mA, power 20% (9 watts), Pass 1 to fixed value. Focal length of the of 2” muse laser machine is 0.68 cm from substrate. From fig 2-35, it is clear that for PMMA substrate, the depth is maximum at focal point and the depth gradually decreases by change in distance between lens and substrate. This is because as the distance between the object and lens increases the spot size increases considerably the length of the cut increases there by reducing the depth. But in case of PMMA the width or length of the cut is minimum which is different from PDMS and Glass. Width of cut is minimum at focal lens and gradually increases with change in lens.

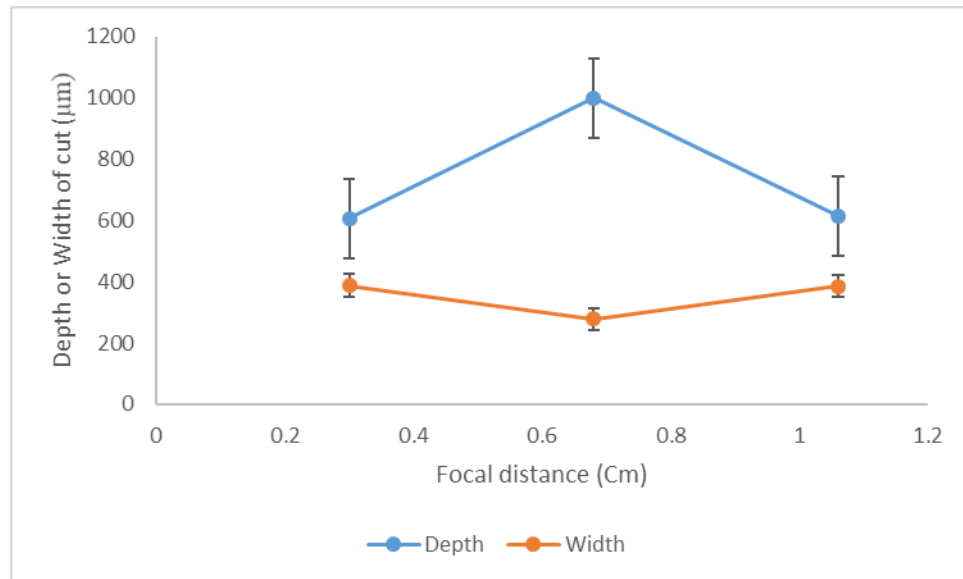


Figure 2-34 Varying focal length at speed 10mm/sec, current 20mA, power 20%



Figure 2-35 Speed 10mm/sec, Power 20% of total power, pass 1 current 20mA focal distance between lens and substrate 0.30 Cm

2.8.3.3 Varying Speed:

Speed is one of the most crucial parameter considered during ablation process. Knowing the effect besides the effect of laser power is vital for understanding the extent of flexibility a CO₂ laser system offers for fabrication. In order to know the effect of speed during laser ablation process, the channel depth as well as width of the channel are investigated. In order to have results that are more consistent the speed of laser machine is generally fixed to a constant value. In this process a PMMA substrate is place exactly at focal length and the speed is varied at 5mm/sec, 10mm/sec, 15mm/sec, 20mm/sec and 25mm/sec there by setting the laser parameters speed 5mm/sec, power 10% of total power, current 20mA, single pass to a constant value. The width of the channel as well as depth are found using optical profilometer and SEM device. Fig 2-37 represents SEM image at speed 5mm/sec, power 10% of total power, current 20mA, single pass at focal length. The results are plotted using Excel sheet. From the results it is

clear that the length of the cut for PMMA almost remained constant at various speed and the depth of the cut gradually decreases with increase in speed. Fig 2-38 represents varying speed of PMMA substrate. This is because when a high-speed laser beam is allowed to pass on the PMMA sheet, the amount of material removed from the substrate is less as the energy imparted on the substrate in a given area is reduced. Due to this, the depth of the cut decreases. Roughness of the channel gradually decreases with increase in speed and thereby decreases by decrease in speed.

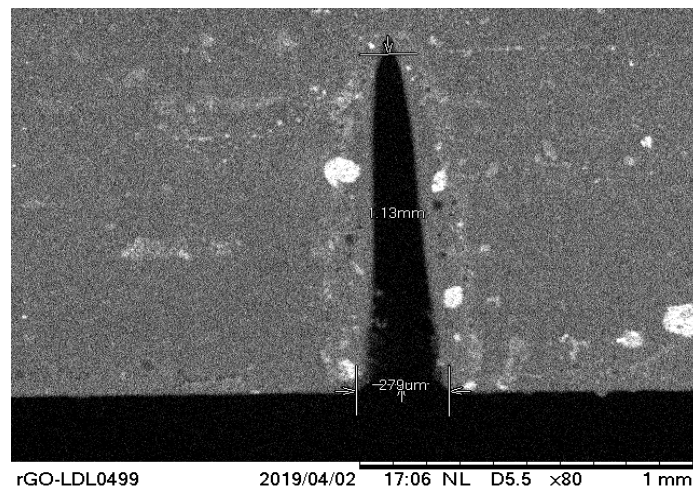


Figure 2-36 PMMA at speed 5, power 10%, current 20, single pass at focal length

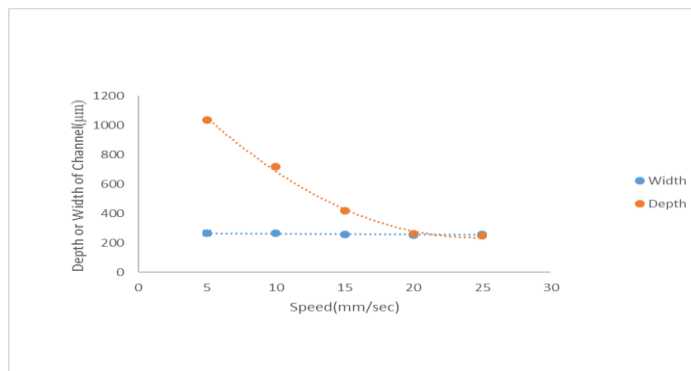


Figure 2-37 Varying Speed at 10% of total power, current (20mA) and passes (1) at focal length

2.8.3.4 Varying Pass:

Figure 2-39 shows the length and the depth of cut by varying passes. During this process, the laser parameters power 10% of total power i.e. 4.5W, current 20 mA, speed 10mm/sec are set to constant value and the passes are varied at focal length. From the figure, the length of the cut remains almost constant while the depth of the cut increases linearly with increase in number of passes. Number of Passes represents X-axis and Y-Axis is represented by width or depth of cut. The maximum depth obtained is 2410 μ m at four pass and the minimum depth obtained is 719.3 μ m at single pass.

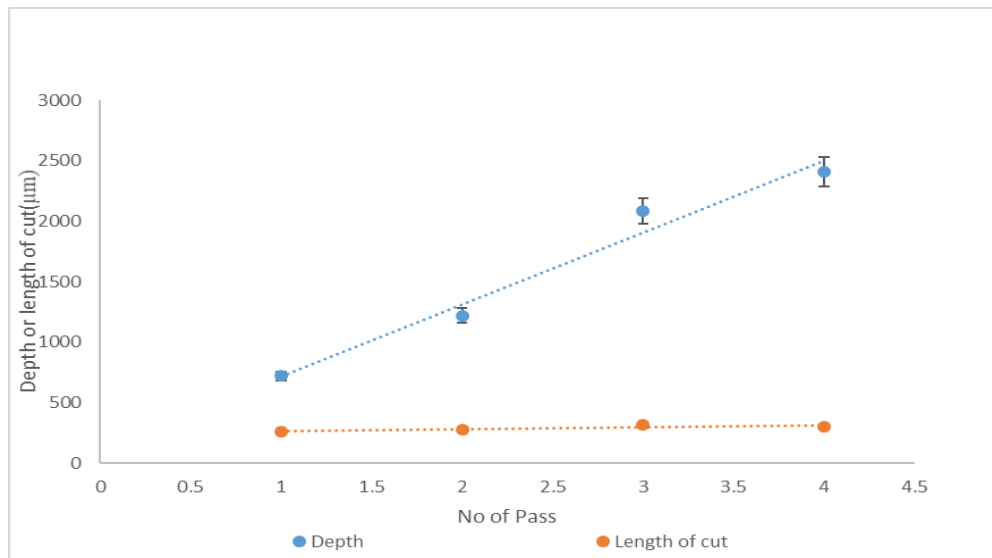


Figure 2-38 Varying Pass at 10% of total power i.e. 4.5W, current 20 mA, speed 10mm/sec

2.8.3.5 Control of shape of cut:

Figure 2-40 shows how varying passes control the shape of the cut of PMMA. By increasing the number of passes the length of the cut remains, same so the depth of the cut varies thus the shape of the cut is controlled.

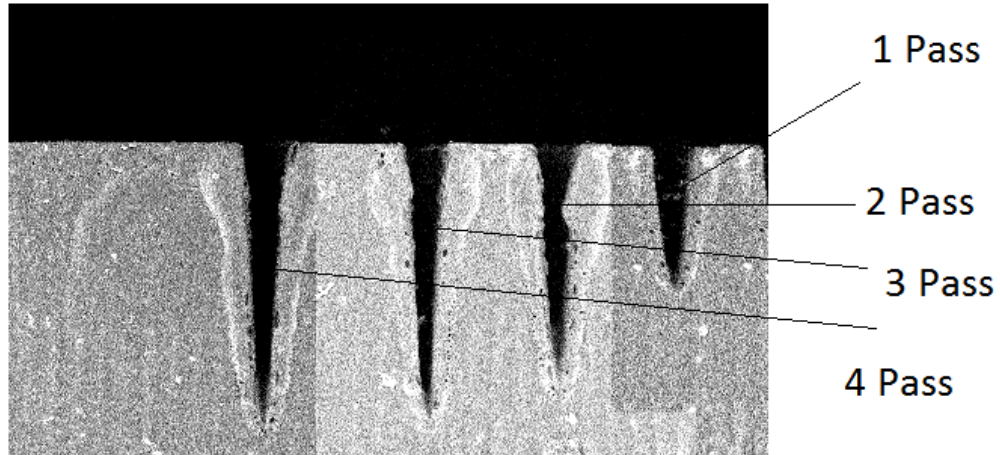


Figure 2-39 Controlling of shape by increasing pass

2.8.4 PDMS

PDMS (Polydimethylsiloxane) is one of the commonly used material for fabrication of microfluids. It has several advantages over other materials as it is inexpensive, transparent, and biocompatible. During this process, PDMS is heated up above evaporation temperature using CO₂ radiation. Due to high heat, top most laser of PDMS surface is ablated. As a result a microfluidic channel is developed. In this process, a PDMS substrate is placed under lens and microfluidic channel is developed by taking one parameter at a time and by putting the rest of parameters as constant. Laser

parameters are Speed, current, power, focal length and pass. Three trails are conducted to have consistent results

2.8.4.1 Varying Power:

Power is one of the crucial parameter in laser system. By varying the power the width of the cut as well as depth varies. In order to know the proper effect of power on PDMS substrate, a microfluidic channel is developed by varying power and by fixing the rest of parameters speed, pass, current to a fixed value at focal length. The width of the channel as well as depth are measured using Scanning Electronic Microscope as well as 3D Optical Profilometer. Figure 2-40 PDMS represents SEM image at 30% of total power, current 20, speed 10, pass 1 at focal length. Power is varied at 10% of total power , 20% of total power, 30% of total power, 40% of total power. Total power of Muse laser machine is 45 W. The rest of the parameters speed, current, pass are set to constant value while varying power (Speed 10mm/sec, current 20mA, Pass 1) at focal point. From the results fig 2-41 it's clear that the depth of the cut is less when compared to Width or length of cut. The length or width of the cut increases linearly with increase in power. This is because increase in percentage of total power increases the amount of heat used to ablated the surface. As a result, the depth as well as length of cut increases. At 5-Watts i.e. 10% of total power we obtained a depth of 182.3333 μm and width of the cut is 528.3333 μm , which is minimum, and the maximum depth is 337 μm and width of the cut is 827.3333 at 40 % of total power

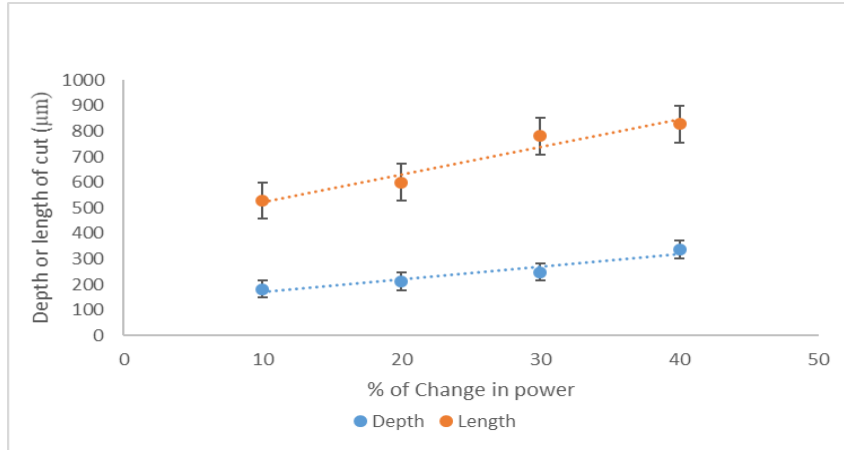


Figure 2-41 PDMS varying power at (Speed 10mm/sec, current 20mA, Pass 1

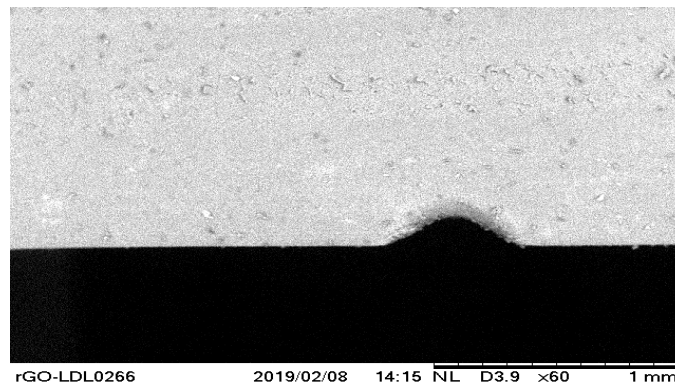


Figure 2-42 PDMS at 30% of total power, current 20, speed 10, pass 1 at focal length

2.8.4.2 Varying Focal length:

Figure 2-43 shows the variation of focal length in terms of depth as well as width of cut. From the figure it is clear that the length or width of the cut is minimum at focal distance (0.68 Cm distance) and the width of the cut gradually increases with increase or decrease in focal distance. This is because when the substrate is placed at focal length, the spot size will be minimum as the beam converges to minimum radius value. The spot

size increases by either increasing or decreasing the distance between focal lens and substrate other than focal distance. As a result as the distance between the object and lens increases the spot size increases considerably the length of the cut increases there by reducing the depth. The depth of the cut is maximum at focal length and the depth of the cut gradually decreases with increase or decrease in focal distance. Here Focal distance is represented on X-Axis in Cm and Length or Width of the cut is represented on Y-Axis in micrometer.

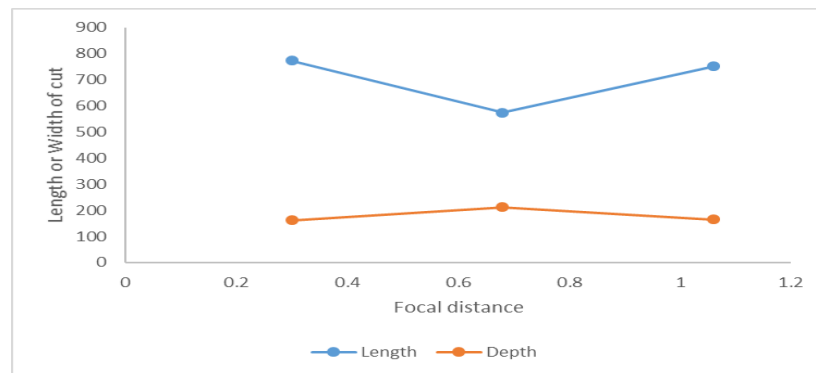


Figure 2-43 Variation of focal distance at at speed 10mm/sec, current 20mA, power 20%

2.8.4.3 Varying Speed:

In order to have consistent results speed of the muse laser machine is generally held fixed during laser micromachining. In order to know how the speed is going to effect the microfluidic device, speed of the laser machine is varied by keeping the rest of parameters as constant. Below figure 2-45 shows that speed is varied at 5mm/sec, 10mm/sec, 15mm/sec, 20mm/sec, 25mm/sec by putting the rest of parameters current at 20 mA, power 5Watts (10% of total power), pass 1 to fixed value. The length of the cut as well as depth of the cut are measured using SEM (scanning electron microscope).

Figure 2-46 says SEM image of PDMS at speed 5, power 10%, pass 1, current 20mA. From the results it is clear that we have maximum depth as well as width of the cut at low speed i.e. 777.333 width at 5mm/sec and 289.6667 depth of the cut at 5mm/sec and the depth of the cut as well as length of the cut decreases with increase in speed. This is because the total amount of heat imparted on the material is less. As the speed is decreased, more amount of heat is imparted on the material, which leads to more length as well as depth of cut. The width of the cut is more when compared to depth when the laser is fired.

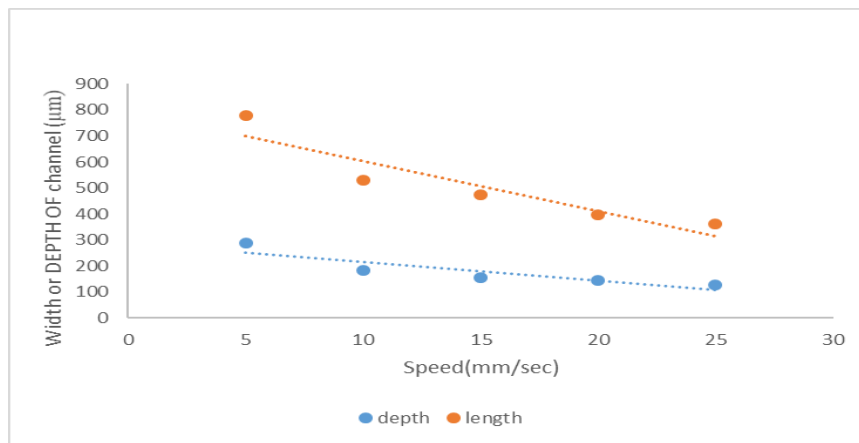


Figure 2-44 PDMS vary in speed at current 20 mA, power 5Watts (10% of total power), pass 1

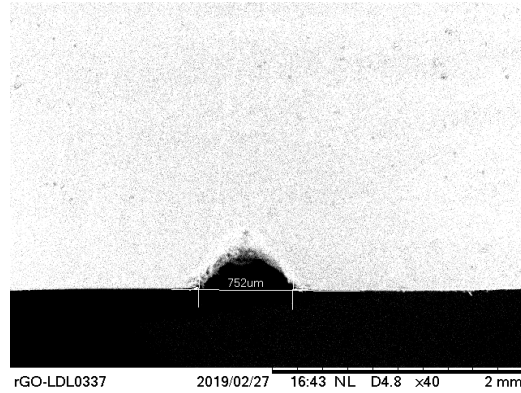


Figure 2-45 SEM image of PDMS at speed 5, power 10%, pass 1, current 20mA

2.8.4.4 Varying Passes:

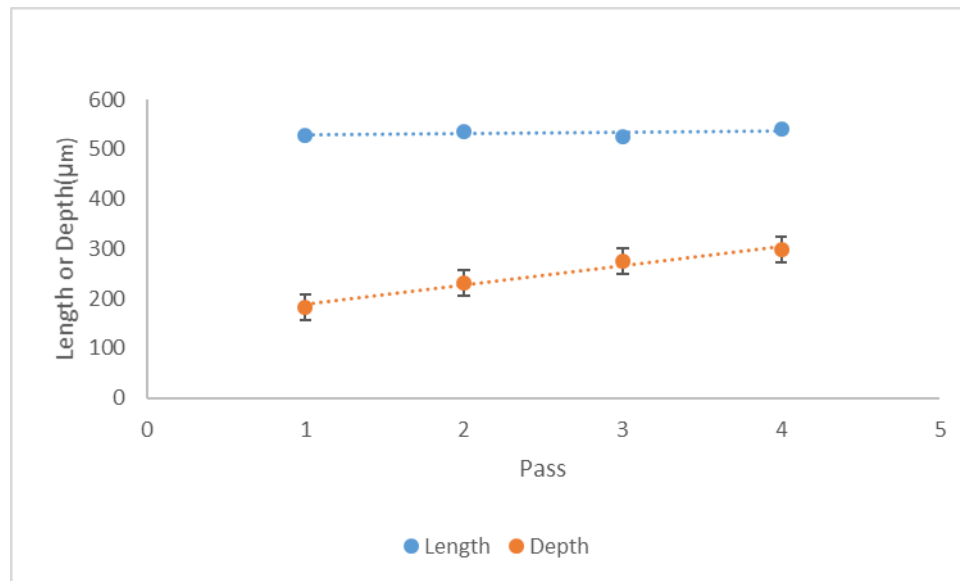


Figure 2-46 PDMS at 10% power, current 20, speed 10mm/sec

Figure 2-47 shows the length of the cut as well as depth of the cut by varying passes and taking the rest of the parameters as constant. Laser machine is varied for single pass, two pass, three pass and four pass and the rest of the parameters are kept to

constant value (10% power, current 20, speed 10mm/sec) at focal length. From the above figure, the length of the cut is almost same for different number of passes. The depth of the cut increases linearly with increase in number of passes. The maximum depth obtained during this process is 298.33 μ m, which is obtained for four passes, and the minimum depth obtained is 182.33 μ m at single pass. The maximum length of the cut obtained during this process is 535.333 μ m at two pass and the minimum length of the cut obtained is 524 μ m at three pass.

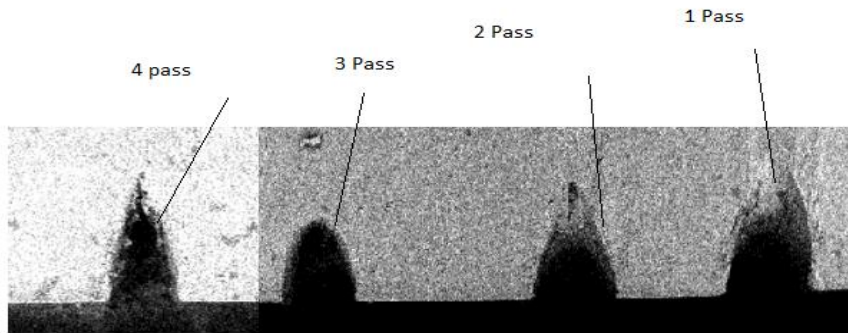


Figure 2-47 Control of shape of cut

Figure 2-48 shows the control of shape of cut for single pass, two pass, three pass and four pass. By increasing the number of passes the length of the cut remains same for PDMS where as the depth of the cut changes thus the shape of the microchannel is controlled.

The depth of the microchannel is exceptionally tunable by repeated ablation on PDMS substrate. As shown in the figure the repeated ablation or multiple pass on same position of substrate creates deeper depth.

2.8.4.5 Roughness Analysis:

In this process, surface analysis is done on the PDMS channel, which is developed by varying speed and taking the rest of parameters Power, Pass, Current to a constant value at focal length. Speed is varied at 5mm/sec, 10mm/sec, 15mm/sec, 20mm/sec, 25mm/sec whereas Power is taken as 10% of total power i.e. 4.5Watts, Current as 20mA, Single Pass and these parameters are fixed to these constant values. The microchannel, which is developed, is measured using 3-D Optical Profilometer in order to obtain surface roughness. Figure 2-48 and 2-50 represents roughness images obtained from profilometer at speed 25mm/sec. Here Sa and Sq values determine the surface roughness. Sa here represents the arithmetic mean height where as Sq represents root mean square value. The roughness data is shown in the form of table below 2-3 for varying Speed by taking rest of parameters as a constant value (Speed= Varied, Current = 20 mA, Pass 1, Power = 10 % of total power = 4.5 Watts at focal length

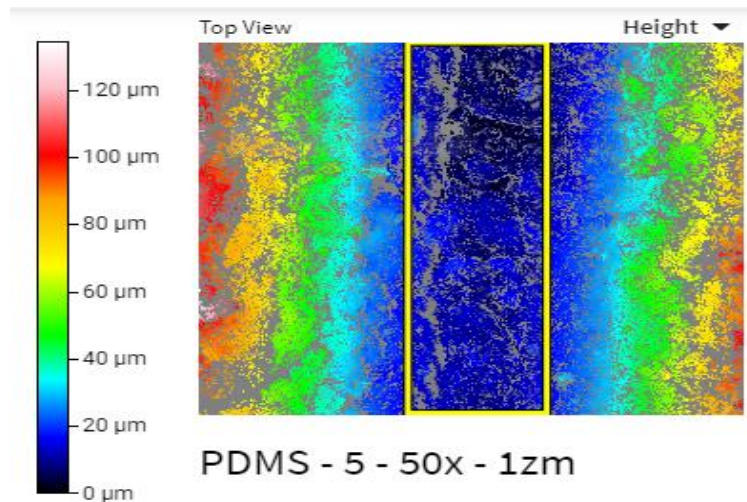


Figure 2-49 Roughness data obtained from profilometer at speed 25mm/sec

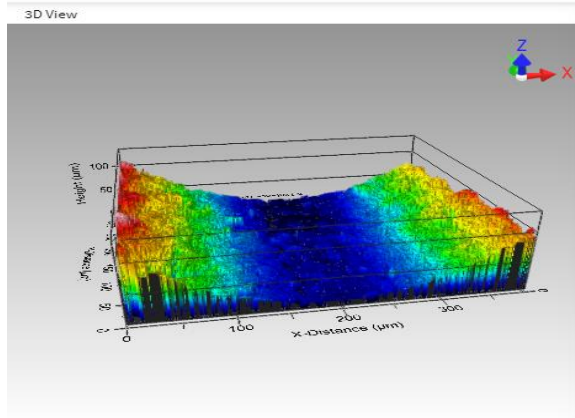


Figure 2-50 3D profilometer image

Table 2-3 Roughness data for PDMS

Varying Speed	Sa (Arithmetical Mean Height)	Sq (Root Mean Square Height)
5mm/sec	1.484 µm	2.158 µm
10 mm/sec	9.625 µm	11.07 µm
15 mm/sec	2.916 µm	3.698 µm

20 mm/sec	7.349 μm	9.235 μm
25 mm/sec	2.183 μm	2.909 μm

PDMS has more roughness at the bottom of channel when compared to those of glass. At 5mm/sec we have the minimum roughness i.e. $S_a=1.484\mu\text{m}$ and $S_q=2.158\mu\text{m}$. The maximum roughness obtained is at 10mm/sec speed i.e. $S_a = 9.625 \mu\text{m}$ and $S_q = 11.07 \mu\text{m}$.

2.9 Comparison of PDMS, PMMA and Glass:

2.9.1 Width of the cut in terms of varying power:

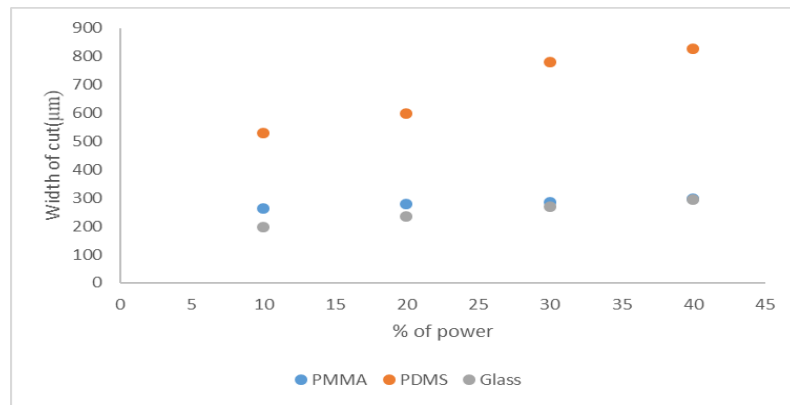


Figure 2-51 Comparison of PDMS, PMMA and Glass by varying power

Figure 2-51 shows the width of the cut of three different materials PMMA, PDMS and Glass by varying percentage of total power. PDMS has more width of the cut when compared to PMMA and Glass. Total power of laser machine is 45 watts. At 10 % of total power i.e. 4.5 Watts PDMS has a width of 777.333 μm which is the highest when compared to other materials, whereas PMMA has 331.1333 μm depth and Glass 211.0667 μm depth. The width linearly increases with increase in percentage of total power for all the three materials and reaches to maximum at 40% of total power. Y-Axis here is represented by width of the cut in (μm) whereas percentage of total power is represented by X-Axis in Watts

2.9.2 Depth of cut in terms of varying power

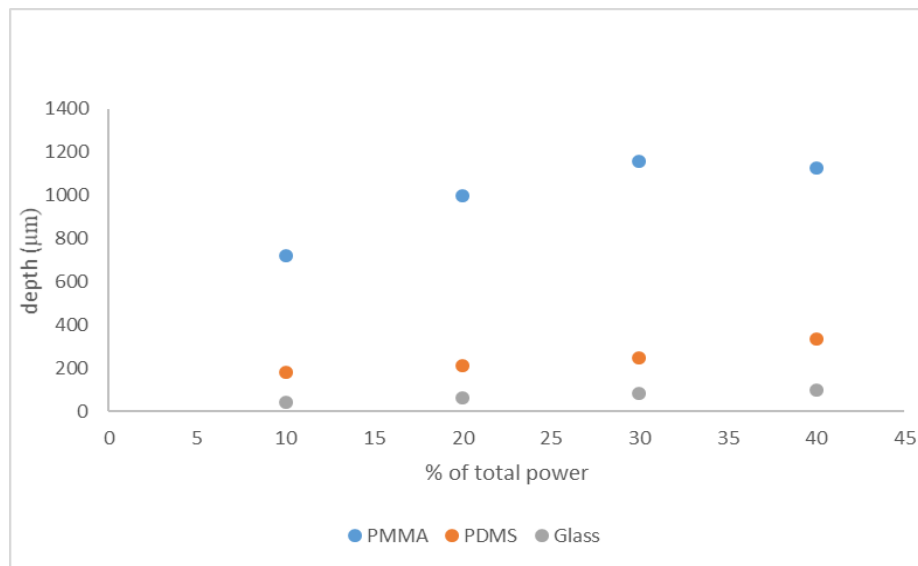


Figure 2-52 Comparison of PDMS, GLASS, PMMA in terms pf depth by varying power
 Figure 2-52 shows the depth of the cut of three different materials PMMA, PDMS and Glass by varying percentage of total power. PMMA has more depth of the cut when

compared to PDMS and Glass. Total power of laser machine is 45 watts. At 10 % of total power i.e. 4.5 Watts PMMA has a depth of 1035.333 μ m which is the highest when compared to other materials, whereas PDMS has only 289.6667 μ m depth and Glass 55.85 μ m depth. The depth linearly decreases with increase in percentage of total power for all three materials and reaches to a minimum of 127.33 μ m for PDMS, 22.14333 μ m for Glass and 246.3333 μ m for PMMA at 40% of power. Y- Axis here is represented by depth of the cut in (μ m) whereas percentage of total power is represented by X-Axis in Watts. .

2.9.3 Width of cut in terms of varying speed

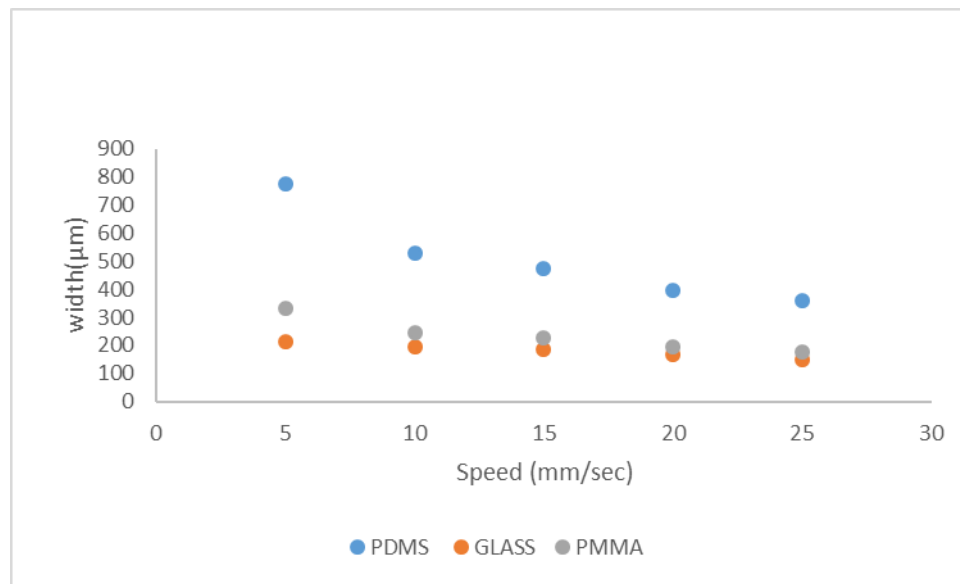


Figure 2-53 Comparison of PMMA, PDMS, and GLASS by varying speed in terms of width

Figure 2-53 shows the width of cut of three different materials PMMA, PDMS, Glass by varying speed (mm/sec). Here Y-Axis is represented by width of the cut in μm and X-Axis is represented by change in speed at 5mm/sec, 10mm/sec, 15mm/sec, and 20mm/sec. From graph, PDMS has highest width of cut i.e. 777.3333 μm followed by PMMA 331.1333 μm , and Glass 211.0667 μm at speed mm/sec. The width of all the three materials linearly decreases with increase in speed and reaches to a minimum of 360.667 μm for PDMS, 147.8667 μm for Glass and 177.8445 μm . Width of cut is represented in micrometer whereas speed is represented in millimeter per second.

2.9.4 Depth of cut interms of varying speed

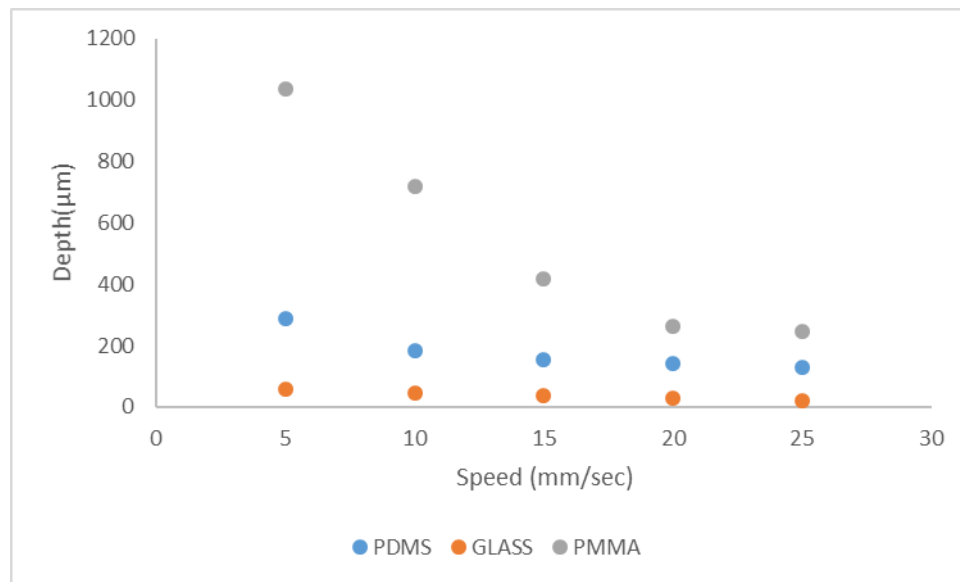


Figure 2-54 Comparison of PMMA, PDMS, GLASS by varying speed in terms of depth. The 2-54 shows the comparison of three different materials PMMA, PDMS and Glass in terms of depth by varying speed. Here depth of the cut is measured in micrometer

whereas speed is varied in millimeter per second. Here X-Axis is represented by speed (mm/sec) and Y- Axis is represented by Depth (μm). From the graph, the depth of the cut gradually decreases with increase in speed and reaches to a minimum value of $127.3333\mu\text{m}$ for PDMS, $246.33\mu\text{m}$ for PMMA and $22.14\mu\text{m}$ for Glass. PMMA has more depth of the cut i.e. $1035.33\mu\text{m}$ at 5mm/sec when compared to other two materials. Glass has the lowest depth of $55.85\mu\text{m}$ when compared to other two materials. The depth of the cut gradually decreases with increase in speed and reaches to a minimum value at 25mm/sec . The depth decreases linearly with increase in speed.

2.9.5 Depth of cut interms of varying focal length

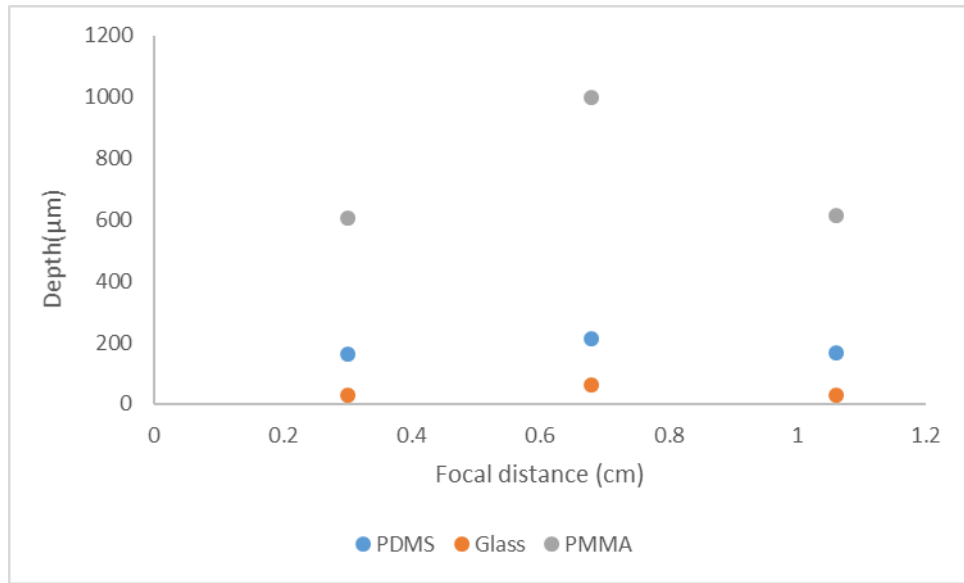


Figure 2-55 Comparisons of PMMA, PDMS and Glass by varying focal length interms of depth

Figure 2-55 shows the comparison of PMMA, PDMS and Glass by varying focal length in terms of depth. Here X- Axis is represented as Focal distance i.e. distance between Lens and substrate and Y-Axis is represented by depth of cut. From the graph, it is clear that the depth of cut will be in maximum at focal length and the depth gradually decreases with increase or decrease in focal lens. PMMA has a maximum depth at focal length i.e. 1000 micrometer followed by PDMS 162 μ m and by Glass i.e. 28.33 μ m.

2.9.6 Width of cut in terms of varying focal length:

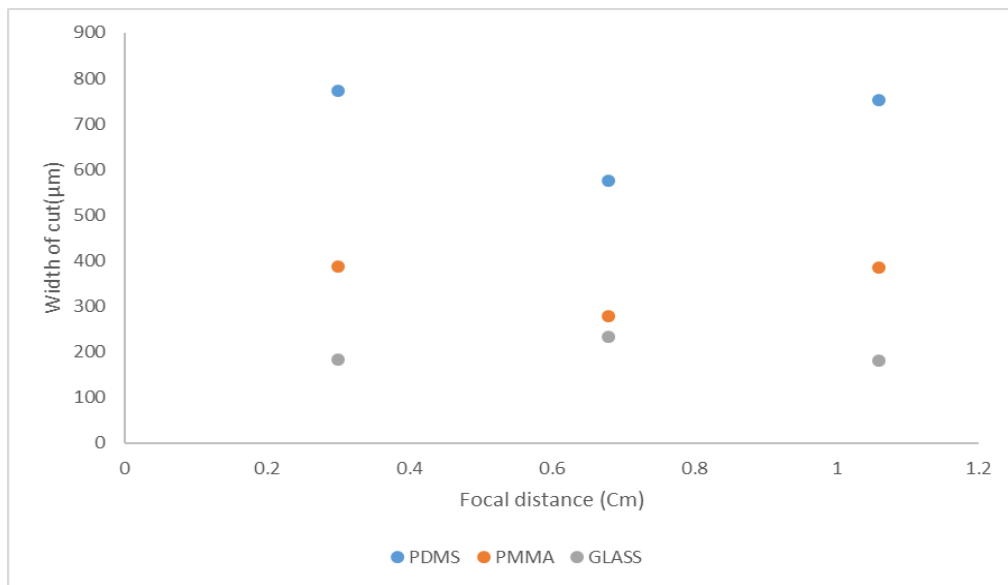


Figure 2-56 Comparisons of PMMA, PDMS, GLASS by varying focal length in terms of width

Figure 2-56 shows the comparison of PMMA, PDMS, Glass by varying focal length in terms of width. PDMS has more width of the cut when compared to other materials next

followed by PMMA and then Glass. From the graph it is clear that width of the cut for both materials PDMS as well as PMMA is minimum at focal length i.e. 0.68 Cm and the width gradually increases with increase or decrease in focal length. For Glass the width is maximum at Focal point and the width gradually decreases with increase or decrease in focal length. Here width of PDMS at focal point is 574.667 μm , for PMMA depth is 278.33 μm , and for Glass it is 233.533 μm . Here focal distance in Cm is taken on X-Axis whereas width of cut in μm is taken of Y-Axis.

2.9.7 Width of cut interms of varying Pass:

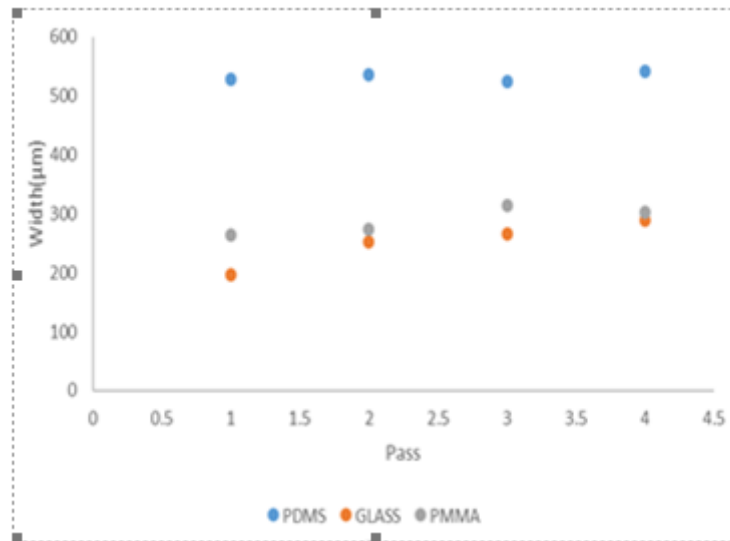


Figure 2-57 Comparison of PMMA, PDMS, Glass at various Pass interms of width of cut

Figure 2-57 shows the comparison of PMMA, PDMS, and Glass by varying passes length in terms of width. X- Axis here represents number of passes whereas Y- Axis here represents width of the cut in micrometer. From the figure, it is clear that PDMS has more width of the cut when compared to PMMA and Glass followed by PMMA and next Glass. The width of the cut for PDMS and PMMA almost remains constant where as for Glass the width slightly increases.

2.9.8 Depth of cut in terms of varying Pass:

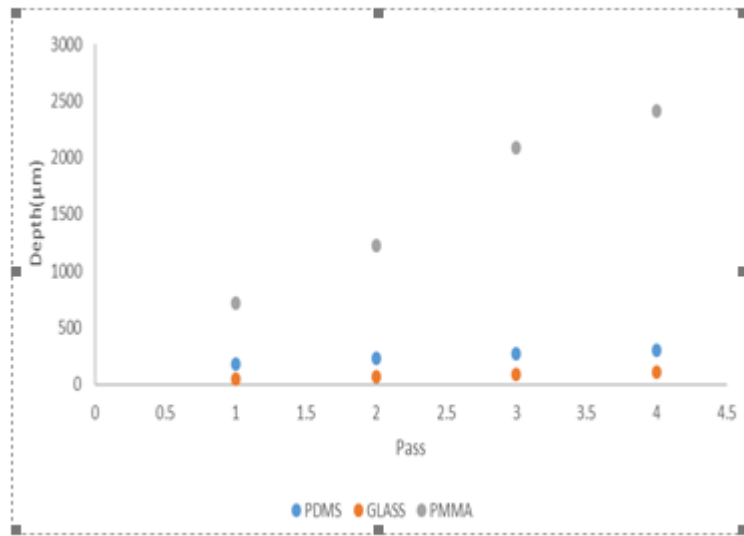


Figure 2-58 Comparison of PMMA, PDMS, GLASS at various Pass interms of Depth of cut

Figure 2-58 shows the comparison of PMMA, PDMS and Glass by varying Pass in terms of depth. Number of Pass represents here X- Axis whereas depth of the cut in micrometer

is represented on Y-Axis. From the graph, it is clear that the depth of cut increases linearly with increase in number of passes. PMMA has rapid increase in depth of cut with increase in pass. The maximum depth of cut obtained for PMMA is 2410 μm whereas for Glass it is 108.7 μm , and for PDMS is 298.33 μm .

2.10 Conclusion:

In this thesis, a microfluidic channel is developed using laser ablation technique. The results show that

1. PDMS has more surface roughness as well as more width of the cut when compared to PMMA and Glass.

2. PMMA has more depth of the cut when compared to PDMS and Glass.

3. Glass has less surface roughness when compared to PDMS.

4. Profile of microchannel can be controlled by increasing the number of passes. Roughness can be reduced by reducing speed.

5. The length or width of the cut is almost same for PDMS and PMMA by varying passes. The depth of the cut increases linearly with increase in speed, power, and number of passes.

6. Depth of the cut is maximum at focal length and the depth gradually decreases with change in focal length.

7.Width of the cut is minimum for PMMA and PDMS at focal length and gradually increases by change in focal distance whereas for Glass the width of the cut is maximum at focal length and the width decreases by change in focal length.

CHAPTER 3

EFFECT OF LASER ON TITANIUM METAL

3.1 Summary

Titanium has numerous applications in engineering, biomedical, biology etc. It is one of the strongest lightweight metal. The goal of this thesis is to investigate the effect of nitriding on a laser textured titanium surface to improve its optical properties for solar thermo photovoltaic application and the objectives are to find the effect of laser assisted groove topography on physical responses of Titanium as well as Attachment of nitrogen on Titanium surface. SEM is used to find topological analysis and XPS is used to find chemical state analysis. The study found that laser textured nitride titanium has better surface properties and increased optical properties when compared to those of non-nitride titanium.

3.2 Introduction

The fast improvement of science and innovation has made an incredible challenge to the execution of materials. Titanium composites or alloys are known as the 'universal metal', and have been generally utilized in aerodynamic and aviation design ascribed to the magnificent properties, for example, low density, high strength, and great corrosive resistance. The titanium nitride (TiN) is a potential useful material because of their metallic and covalent binding attributes. It shows great similarity with semiconductor industry and conventional or traditional silicon devices as Ohmic contact layer, diffusion

barrier, sensor material, turn electron materials, and straightforward conductive layer in photovoltaic industry. Titanium is one of the fourth most abundant element on the earth. Titanium being lightweight has many advantages when compared to other metals in terms of strength, as it is one of the strongest metal on this planet. In reality, titanium has the highest strength-to-density ratio when compared to other metallic elements on periodic table[3]. Another key advantage of titanium is its natural resistance corrosion as well as rust. If a metal is exposed to moisture or air, it undergoes some chemical reactions known as oxidation, which can subsequently lead to corrosion. Titanium whether used in indoor or outdoor has natural resistance to this phenomenon so that it can last long for years without undergoing any rust or corrosion[32].

3.2.1 Applications of Titanium:

1. Titanium is used in compressor blades and hydraulic system components. Titanium 6AL-4V is used in aircraft applications.

2. Due to their high corrosion resistance, titanium alloys are used in aircraft, armour plating, missiles, spacecraft and naval ships.

3. Titanium is also used in some critical structural parts, landing gear, firewalls hydraulic systems and exhaust ducts (helicopters) when alloyed with vanadium and aluminum. In reality, about two thirds of titanium metal is used in frames and aircraft engines.

4. As titanium is biocompatible and environmental friendly, titanium is used in medical filed as surgical implants as well as surgical implements. Titanium has the property to Osseo integrate, which helps use of titanium in dental implants.

5. Titanium being a metal has many applications in aerospace, industrial, architectural and medical applications. Titanium alloys are also used in engines and airframes. They are also used in power generation, airframes, chemical processing, petroleum, computer industry, automotive industry, human implants, photovoltaic cell etc.

3.2.2 Laser applications on titanium:

Laser has numerous applications on titanium some of them are:

1. Titanium grooves are used as a bone implant in animal surgery
2. Laser is used on titanium on Aerospace applications for heavy fatigue testing[32]

3.2.3 Plasma Nitriding on Titanium.

Laser generally on titanium alloy creates bulges, Cracks on the surface of walls. In order to remove or minimize those cracks and bulges Plasma nitriding treatment is applied on the titanium alloy. Ming-Zheng Wang investigated on effects of combined treatment of plasma nitriding and laser surface texturing on vacuum tribological behavior of titanium alloy and found that plasma nitriding enhances the wear resistance of titanium as well as decreases coefficient of friction of titanium by making surface textures of titanium alloy. He also found that plasma nitriding can increase strength of titanium alloy there by reducing the plastic deformation as well as adhesive wear of titanium alloy during friction[33]. Morshed Khandaker investigated roughness, biocompatibility, and hardness by applying plasma on titanium and found that nitrogen plasma treatment changes the surface roughness as well as chemical properties of titanium alloy when compared to the

untreated samples. He also found that it reduces bulges and cracks that are created by laser grooves, which increases the strength as well as compatibility[33].

3.3 Materials and Methods:

TC4(Ti-6Al-4V) titanium sheets are cut into 10 X 10 mm and are polished using 3 steps of polished liquid MetaDi supreme Polycrystalline diamond Suspension to obtain a roughness less than 100 μ m. Figure 3-1,3-2,3-3 shows different sets of titanium samples



Figures 3-1 Titanium Round samples

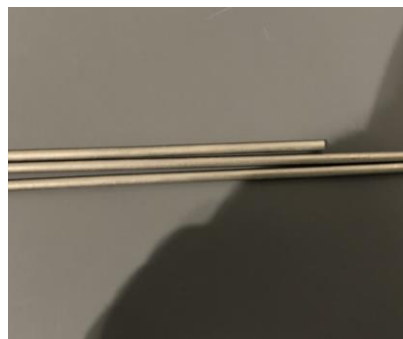


Figure 3-2 Titanium Rods



Figure 3-3 Titanium Flat samples

3.3.1 Sample Preparation:

Surface textures were created on titanium Ti-6Al-4V alloy flat samples using high power full spectrum laser. Three groups of Flat samples are prepared

1. Controlled
2. Laser Treated
3. laser plus TiN treated Ti (ITiN)

Samples are well polished. After polishing all the titanium samples are cleaned using four steps (Branson, Ethanol, Acetone, and Water) in ultrasonic cleaner. A Titanium sample without groove is called as control sample. Laser pulses from high power Full spectrum laser were applied on titanium flat surface to create continuous linear microgrooves for ITi samples. Using plasma nitrogen deposition system the laser textured titanium samples are exposed to nitrogen gas for ITiN samples. The surface characteristics as well as chemical states are analyzed using XPS analysis.

3.3.2 Chemical state evaluation by X-ray photoelectron spectroscopy (XPS):

The chemical changes on titanium 10x10mm flat sample after treated with nitrogen plasma are evaluated by XPS (X-ray photoelectron spectroscopy). The XPS system usually consists of integrated 5keV electron gun used for Auger excitation and an X-ray tube with usually consists of Mg and Al sources. The Al source was used for the analysis. Scans were completed in a step mode utilizing Al K α radiation at 13 kV and 12 mA X-ray power. Survey scans were completed using 500 ms withstand time with 0.5 e V step and the high resolution detailed scans are done using 1000 ms withstand time and 0.1 eV step size. TiN and TiOxNy arrangement or formation after plasma treatment and binding energies around N1s, O1s, and Ti2p peaks were evaluated. Figure 3-4 shows X-ray photoelectron spectroscopy machine located at Admore, Oklahoma.

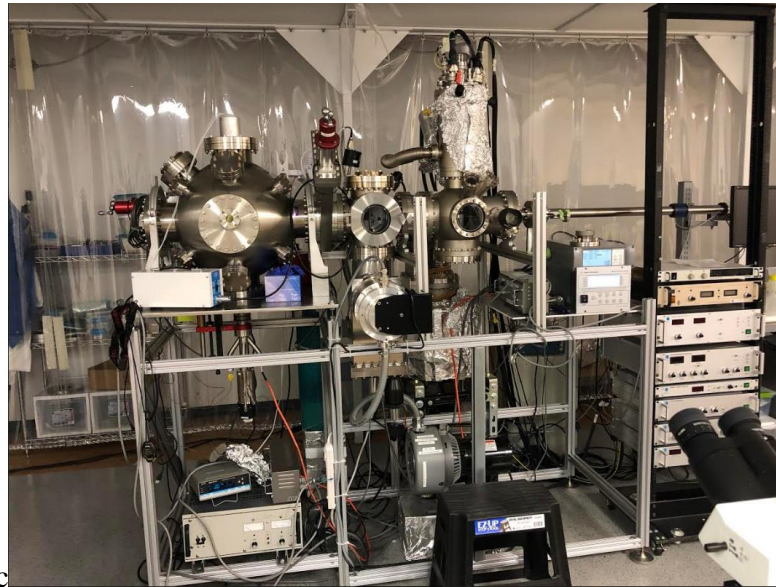


Figure 3-4 X-ray photoelectron spectroscopy machine Admore, Oklahoma

3.4 Results:

3.4.1 Topographic analysis:

The laser surface textures, which are made on the titanium, sample using high power full spectrum laser are topologically analyzed using SEM (Scanning Electronic Microscope) machine. Figure 3-5, 3-6 shows the length, depth as well as distance between grooves. The depth obtained during surface texturing is $168\mu\text{m}$, the distance between grooves is $243\mu\text{m}$, and the width of the cut is $105\mu\text{m}$.

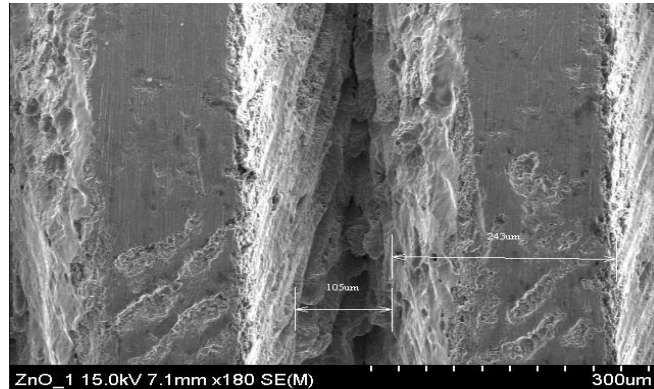


Figure 3-5 determining length and distance between grooves

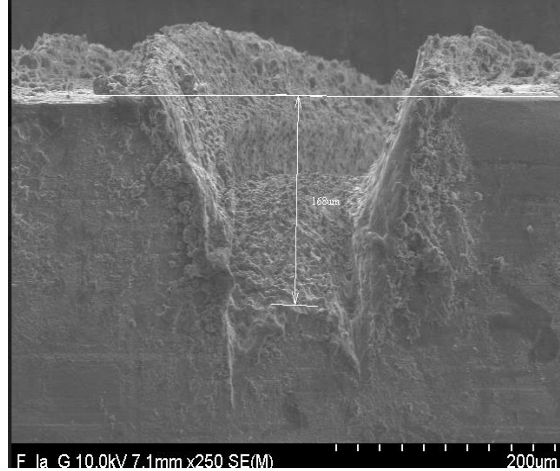


Figure 3-6 determining depth of the groove

3.4.2 Chemical state analysis:

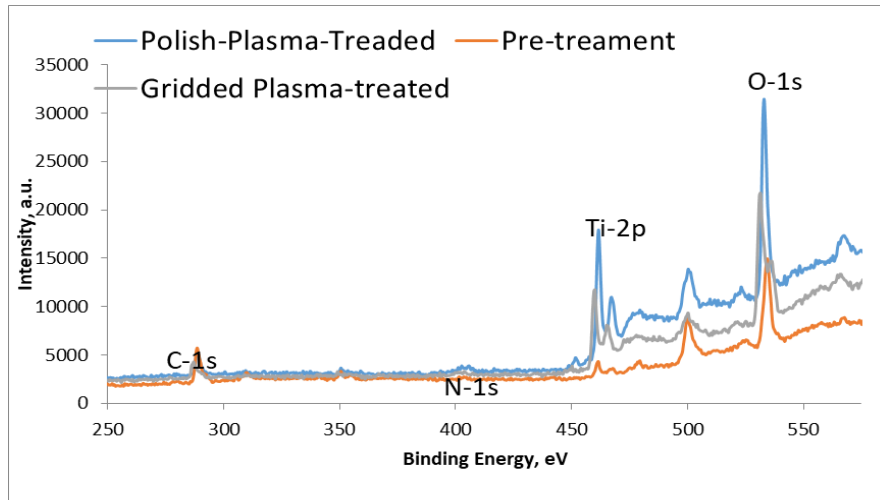


Figure 3-7 XPS analysis of Polished plasma treated, Pre treatment, gridded plasma treated for titanium alloy

Chemical state analysis is carried out using XPS analysis. XPS analysis before and after nitrogen plasma treatment revealed successful coating of plasma nitride on Titanium surface. Figure 3-7 shows the binding energy and intensity values for polished plasma titanium sample. Binding energy is taken and X-Axis and Intensity on Y-Axis. Native oxides are still present on samples and cannot be removed as the titanium samples are treated with plasma. As the native oxides are not removed, there is a presence of O-1s and Ti2p. A small amount of carbon C-1s is observed which says the formation of carbide compounds and small amount of nitrogen is absorbed on the graph, which says the presence of nitrogen on the sample. From the figure it is clear that Plasma nitrated titanium samples has higher binding energy and low HRC compared to those of titanium samples which are not plasma nitride.

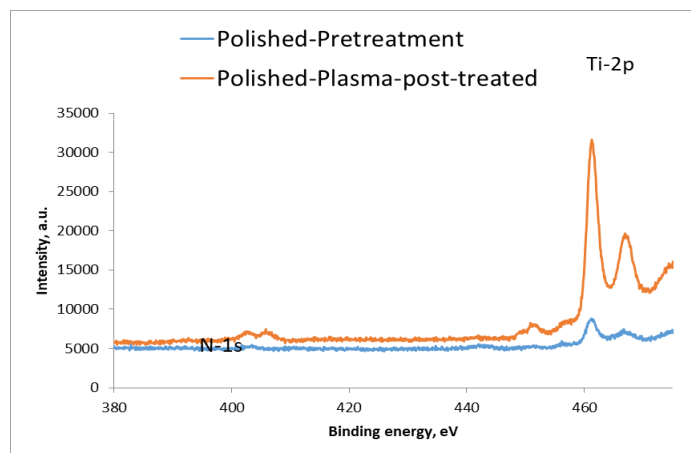


Figure 3-8 Polished pretreatment and polished plasma post treated titanium sample

Figure 3-8 shows the polished pretreatment and polished plasma post treated sample. From the figure Native oxides are found on Polished Plasma post treated sample as the plasma is applied on the titanium sample and no steps are taken to remove native oxides other than cleaning with ethanol. So Ti-2p is observed in the graph which is a native oxide. There is a formation of N-1s in the figure which tell us the titanium samples has small amount of nitrogen. In case of polished pretreatment there is no formation of native oxides as the samples are neatly and necessary steps are taken to remove them.

3.4.3 Surface Analysis:

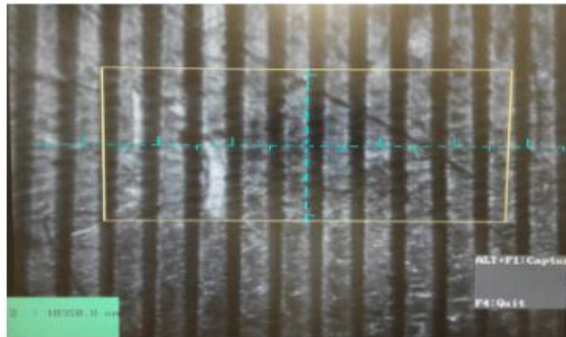


Figure 3-9 Profiler camera picture

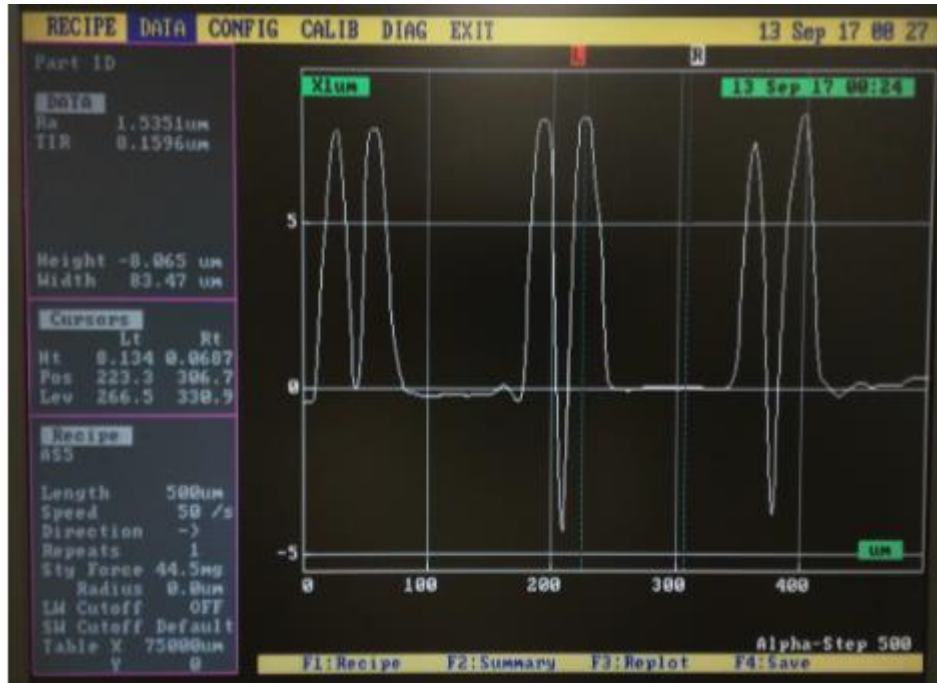


Figure 3-10 Surface view of sample

Profiler images are taken in order to do the surface analysis. Figure 3-09 represents profiler camera picture of sample and figure 3-10 represents surface image of sample. Middle peaks are 8µm high with a -4.4µm dip in between the two. Peaks generally represents roughness in the sample. Multiple scans are conducted to determine roughness. From the results, it is found that laser texturing is creating more roughness on the sample.

3.5 Conclusion:

1. In order to know the effect of nitrogen on titanium XPS analysis is carried out. From the results it is found that Nitriding has positive influence on the surface characteristics. Nitriding makes the laser grooved Ti surface more reflective compared to those of non-nitriding Ti surface.

2. Plasma nitriding is applied on titanium rods to remove bulge formation as well as cracks on walls.

3. From Topographic analysis the depth obtained during surface texturing is $168\mu\text{m}$, the distance between grooves is $243\mu\text{m}$, and the width of the cut is $105\mu\text{m}$.

4. Laser grooving creates more roughness on titanium sample.

CHAPTER 4

4.1 Conclusion:

In this thesis, a microfluidic channel is developed using different laser parameters. The results shows that PDMS has more surface roughness as well as more width of the cut when compared to PMMA and Glass. PMMA has more depth of the cut when compared to PDMS and Glass. Glass has less surface roughness when compared to PDMS. Profile of microchannel can be controlled by increasing the number of passes. Roughness can be reduced by reducing speed. The length or width of the cut is almost same for PDMS and PMMA by varying passes. The depth of the cut increases linearly with increase in speed, power, and number of passes. Depth of the cut is maximum at focal length and the depth gradually decreases with change in focal length. Width of the cut is minimum for PMMA and PDMS at focal length and gradually increases by change in focal distance whereas for Glass the width of the cut is maximum at focal length and the width decreases by change in focal length.

In order to know the effect of nitrogen on titanium XPS analysis is carried out. From the results it is found that nitriding has positive influence on the surface characteristics. Nitriding makes the laser grooved Ti surface more reflective compared to those of non-nitriding Ti surface. Plasma nitriding on titanium removes grooves as well as bulges across walls. From Topographic analysis the depth obtained during surface texturing is 168 μm , the distance between grooves is 243 μm , and the width of the cut is 105 μm .

4.2 Future work:

For Polymers

1. Hydrophobicity for microfluidic device can be found
2. Roughness analysis for PMMA can be determined
3. Spot size by varying parameters can be determined

For Titanium metal:

1. Surface roughness can be determined
2. Refractive index can be found

4.3 References:

- [1] "MICROFLUIDICS: A GENERAL OVERVIEW OF MICROFLUIDICS," in *Elveflow*, ed.
- [2] T. Betancourt and L. J. I. j. o. n. Brannon-Peppas, "Micro- and nanofabrication methods in nanotechnological medical and pharmaceutical devices," vol. 1, no. 4, p. 483, 2006.
- [3] M. R. H. Matthew Benton, Prashanth Reddy Konari, Sanjeewa Gamagedara, "Effect of Process Parameters and Material Properties on Laser Micromachining of Microchannels."
- [4] *Disadvantages of Infrared Waves*. Available: <http://www.edurite.com/kbase/disadvantages-of-infrared-waves>
- [5] H. Klank, J. P. Kutter, and O. J. L. o. a. C. Geschke, "CO₂-laser micromachining and back-end processing for rapid production of PMMA-based microfluidic systems," vol. 2, no. 4, pp. 242-246, 2002.
- [6] B. D. N. G. a. G. O'Connor, "Laser-Based Fabrication for Microfluidics Devices on Glass for Medical Applications," *IntechOpen*, 2016.
- [7] P. S.-M. Indalesio Rodriguez, Christopher L. Kuyper., "Rapid prototyping of glass microchannels," 2002.
- [8] S. Cheriyaedath, "News-Medical life sciences," ed, 2018.
- [9] *MICROFLUIDICS: A GENERAL OVERVIEW OF MICROFLUIDICS*. Available: *MICROFLUIDICS: A GENERAL OVERVIEW OF MICROFLUIDICS*
- [10] M. Hauer, T. Dickinson, S. Langford, T. Lippert, and A. Wokaun, "Influence of the irradiation wavelength on the ablation process of designed polymers," *Applied Surface Science*, pp. vol. 197-198, pp. 791-795, 2002.

- [11] N. Naik *et al.*, "Microfluidics for generation and characterization of liquid and gaseous micro-and nanojets," vol. 134, no. 1, pp. 119-127, 2007.
- [12] C. J. I. M.-L.-. Ilescu, "Microfluidics in glass: technologies and applications," vol. 36, no. 4, p. 204, 2006.
- [13] B. Ziaie, A. Baldi, M. Lei, Y. Gu, and R. A. J. A. d. d. r. Siegel, "Hard and soft micromachining for BioMEMS: review of techniques and examples of applications in microfluidics and drug delivery," vol. 56, no. 2, pp. 145-172, 2004.
- [14] M. J. Madou, "Fundamentals of microfabrication: the science of miniaturization," *CRC Press LLC*, p. 2nd edition, 2002.
- [15] Y. X. a. G. M. Whitesides, "SOFT LITHOGRAPHY," *Annual Reviews*, p. Volume 28, 1998.
- [16] M. C. Gower, "Industrial applications of laser micromachining," *Opt Express*, vol. 7, no. 2, pp. 56-67, Jul 17 2000.
- [17] "Carbon Dioxide (CO₂) Lasers Information," ed: Engineering 360 powered by IEEE.
- [18] *What is Laser Ablation?* Available: <https://appliedspectra.com/technology/laser-ablation.html>
- [19] J. Rodrigues, "Innovative and an Effective Fiber Optic probe for Laser Ablation of tumors," *Health & Medicine*, 2018.
- [20] "Laser ablation," *Wikipedia, the free encyclopedia*.
- [21] "Laser processing, ablation and deposition," Available: http://www.iqfr.csic.es/ql/Web_QL_english/Ablacion_laser/AL_home_data/AL_Lineas_Investigacion/AL_LI_Lpad.html.
- [22] a. a. r. Mike. *Laser Ablation Applications*. Available: <https://www.spilasers.com/application-ablation/laser-ablation-applications/>
- [23] T. Wang, J. Chen, T. Zhou, and L. J. M. Song, "Fabricating Microstructures on Glass for Microfluidic Chips by Glass Molding Process," vol. 9, no. 6, p. 269, 2018.
- [24] M. Imran, R. A. Rahman, M. Ahmad, M. N. Akhtar, A. Usman, and A. J. L. P. Sattar, "Fabrication of microchannels on PMMA using a low power CO₂ laser," vol. 26, no. 9, p. 096101, 2016.
- [25] T. N. Kim, K. Campbell, A. Groisman, D. Kleinfeld, and C. B. J. A. P. L. Schaffer, "Femtosecond laser-drilled capillary integrated into a microfluidic device," vol. 86, no. 20, p. 201106, 2005.
- [26] D. B. Wolfe, J. B. Ashcom, J. C. Hwang, C. B. Schaffer, E. Mazur, and G. M. J. A. M. Whitesides, "Customization of poly (dimethylsiloxane) stamps by micromachining using a femtosecond - pulsed laser," vol. 15, no. 1, pp. 62-65, 2003.
- [27] R. Suriano *et al.*, "Femtosecond laser ablation of polymeric substrates for the fabrication of microfluidic channels," vol. 257, no. 14, pp. 6243-6250, 2011.
- [28] D. Snakenborg, H. Klank, J. P. J. J. o. M. Kutter, and microengineering, "Microstructure fabrication with a CO₂ laser system," vol. 14, no. 2, p. 182, 2003.

- [29] T.-F. Hong *et al.*, "Rapid prototyping of PMMA microfluidic chips utilizing a CO₂ laser," vol. 9, no. 6, pp. 1125-1133, 2010.
- [30] J.-Y. Cheng, C.-W. Wei, K.-H. Hsu, T.-H. J. S. Young, and A. B. Chemical, "Direct-write laser micromachining and universal surface modification of PMMA for device development," vol. 99, no. 1, pp. 186-196, 2004.
- [31] "The World's First \$19k 3D Profilometer: The Profilm3D," ed: FILMETRICS.
- [32] "What are Pros and Cons of titanium?," in *Monroe*, ed, 2016.
- [33] "Titanium Applications," in *Continental steel and tube company*, ed.